ORIGINAL RESEARCH

A novel collapse prediction index for voltage stability analysis and contingency ranking in power systems

Salah Mokred[1], Yifei Wang[1*] and Tiancong Chen[2]

Abstract

Voltage instability is a serious phenomenon that can occur in a power system because of critical or stressed conditions. To prevent voltage collapse caused by such instability, accurate voltage collapse prediction is necessary for power system planning and operation. This paper proposes a novel collapse prediction index (*NCPI*) to assess the voltage stability conditions of the power system and the critical conditions of lines. The effectiveness and applicability of the proposed index are investigated on the IEEE 30-bus and IEEE 118-bus systems and compared with the well-known existing indices (L_{mn}, *FVSI*, *LQP*, *NLSI*, and *VSLI*) under several power system operations to validate its practicability and versatility. The study also presents the sensitivity assumptions of existing indices and analyzes their impact on voltage collapse prediction. The application results under intensive case studies prove that the proposed index *NCPI* adapts to several operating power conditions. The results show the superiority of the proposed index in accurately estimating the maximum load-ability and predicting the critical lines, weak buses, and weak areas in medium and large networks during various power load operations and contingencies. A line interruption or generation unit outage in a power system can also lead to voltage collapse, and this is a contingency in the power system. Line and generation unit outage contingencies are examined to identify the lines and generators that significantly impact system stability in the event of an outage. The contingencies are also ranked to identify the most severe outages that significantly cause voltage collapse because of the outage of line or generator.

Keywords Voltage stability indices, Voltage collapse, *NCPI*, Weak buses and critical lines, Maximum load-ability, Contingency ranking and analysis

1 Introduction

Voltage instability is one of the significant problems in the electricity system that needs to be considered to secure power transfer to consumers. Because of a continuous increase in electrical load the present-day electrical power system urgently requires secure electrical power

*Correspondence:
Yifei Wang
wyf@seu.edu.cn
[1] Electrical Engineering Department, Southeast University, Nanjing 210096, China
[2] Electromechanical Engineering School, Zhongyuan Institute of Science and Technology, Zhengzhou 450007, China

transmission facilities. From an environmental and economic point of view, it is challenging to install new transmission lines. Also, the situation becomes more complex with the increasing penetration of renewable energies. The most crucial challenge facing the network is excessive loading in transmission lines resulting in a massive voltage drop, which can cause voltage collapse due to overload on the lines. In this case, the line becomes in a critical state, and the system can face collapse under even small disturbances [1–4]. Voltage collapse leads to the exit of a line from the system when the loading exceeds the allowable limit. Subsequently, the exiting of the line from the system increases the power flow in other lines,

potentially causing consecutive exits of the lines and leading to the blackout of the entire network.

Voltage stability is defined as the capability of an electric power system to preserve an acceptable voltage at all the buses of the grid during normal operation and after being exposed to disturbances [5]. A heavily loaded power system is one of the most critical factors in creating voltage instability [6]. One of the most important reasons for the collapse of voltages is the inability of an electric power system to provide sufficient reactive power because of excessive reactive power consumption by the loads or the system itself. Because of numerous voltage collapses occurring in several countries over the past few decades, the voltage stability problem has gained extensive attention. On July 12, 2004, voltage instability caused the splitting of the south part of the Hellenic power system from the system resulting in a 4.5 GW total load without power [7]. In the North American and European systems, approximately 63 GW of the load was interrupted because of outages of 531 generation units and over 400 transmission lines [8].

There are several analytical techniques, described in the literature, for measuring the voltage stability and loading margin of the current operating condition, with voltage stability indices making up the majority of these measurements. [9, 10] use the P–V and Q–V curves at certain load buses to determine the stability margin. This technique illustrates the limit of the minimal voltage magnitudes and the maximum active/reactive power required. In order to evaluate the entire status of voltage stability, reference [11] suggests the generalized global voltage stability margin (GVSM) idea using an equivalent pi-network. However, the methods in [9–11] are significantly time-consuming. In [12], a stability index based on Thevenin's impedance to load impedance ratio is suggested. When only active power is being loaded, the impedance ratio approach finds the voltage collapse point before other methods. However, it takes longer to find the bifurcation point when reactive power is being loaded. The multi-objective biogeography optimization technique is used in [13] to diagnose the weak segments and buses of the grid responsible for voltage collapse. A stability factor based on the single line equivalent of a power system is proposed in [14]. This index presents a nonlinear property and a very high sensitivity close to the critical region. Therefore, it is hard to estimate the instability prediction accurately.

Reference [15] proposes a line collapse proximity index for collapse prediction while [4, 16] compare and evaluate some line voltage stability indices. However, not all probable operating scenarios in power systems are considered. In [17], it concludes that identifying the weak buses in power systems is very important to support

them with Var sources to avoid voltage collapse, and thus a high-performance prediction index is required.

Static and dynamic stability bifurcations have been recognized as contributing factors to voltage collapse in various electric power system models [18–25]. An L-index is created in [26] based on the normal load-flow solution, and is appropriate for loads with constant power. However, the L-index-based approach gives an incorrect solution when the load is not a constant power type [27]. Collapse prediction in contingency N-1 is studied in [28] using a recurrent neural network, whereas [29, 30] use an artificial neural network (ANN) for an online assessment of voltage security. However, these methods need massive neural network training to obtain a solution for actual operating conditions, and this may not be appropriate for a large power grid. Moreover, the approach is susceptible to topological changes.

The voltage stability index of each power transmission line is an effective measure for power system monitoring [31]. Power system operators and researchers have been continuously interested in performance indices to predict the closeness of the system to the voltage instability boundary. This is because they can be used online or offline to assist system operators in determining how close the system is to a potential voltage instability situation [32]. The dimension measurement from the base-case operating point to the critical level (voltage collapse point) is used by the static voltage stability indices [33–40], while [38] delineates and classifies almost 40 voltage stability indices over the past 3 decades. From different viewpoints, the critical boundary index CBI proposed in [39] relies on active and reactive power variations. However, CBI takes more time than conventional VSIs.

A thorough review of 49 different VSIs is presented in [41], which lists each index's benefits and drawbacks separately. Based on the ideal location of reactive power support, reference [42] employs the Differential Evolutionary approach to determine the vulnerable spots in a large grid, while [43] proposes an index based on reactive power loss. Since only the loss of reactive power is considered while the impact of active power loss (which can significantly affect voltage stability) is ignored, this method may produce erroneous results. Bus and line stability indices are used in [44–50] to monitor the closeness of the power system to voltage instability. [44–51] conduct in-depth research on several real-time monitoring techniques, including a phasor measurement unit (PMU) and machine learning based on voltage stability indices. A sudden rise in load, technical problems, improper operation of voltage control equipment, and the failure of a generating unit are some factors that may cause voltage collapse [52, 53]. Voltage instability can also occur when there is

an imbalance between the supply and demand for reactive power. The series compensation technique is more effective than shunt compensation in preventing voltage instability under various power factors when both active and reactive power are extremely close to threshold levels in the system [54–57].

Currently, many studies focus on incorporating the line voltage stability indices (LVSIs) in the traditional optimal power flow problems for multi-objective optimization (MOOP) [58–65], and aim to select a high-performance index of LVSIs to improve system stability [60]. Also, [60] concludes that the voltage stability indices have applicability in planning voltage stability improvement for a grid that integrates renewable energy sources (RES).

Moghavvemi and Omar [66] proposes the line stability index (L_{mn}) to measure the critical cases of lines. In [67], the voltage collapse points and contingency rankings of crucial lines are estimated using the fast voltage stability index (*FVSI*). However, the indices L_{mn} [66] and *FVSI* [67] provide erroneous collapse prediction results under specific operating situations since they do not consider the active power flow. Using a load flow solution, the line stability factor (*LQP*) is created in [68] to assess the lines' voltage stability state. However, the *LQP* index entirely ignores the line resistance and assumes that the lines are lossless. In addition, the *LQP* index does not consider the influence of active and reactive power flow directions. *NLSI* is proposed in [69], and ignores the difference in voltage angles of the sending and receiving buses, while *NLSI* also does not consider the influence of active and reactive power flow directions.

Under some operating scenarios, *NLSI* fails to predict the collapse, especially under heavy active power conditions. The *NVSI* index [70] uses a simplified transmission line model, which entirely ignores the resistance of the transmission line, resulting in inaccurate predictions when the resistances of branches are high. The Thevenin equivalent circuit and a two-node arrangement are used in [71] to formulate the index *VSLI* which has high performance in the case of heavy apparent power load since it doesn't ignore any variables except the line shunt admittance. Nevertheless, *VSLI* fails to predict the collapse in some instances when there is heavy reactive power.

The contributions of this paper are:

1. A new stability index is proposed, namely, the novel collapse prediction index (*NCPI*).
2. The proposed *NCPI* index accurately determines the points of voltage collapse, the weak buses in the power systems, the most critical lines, the maximum load-ability in each particular bus and the most sensitive lines due to line or generator outage contingency.

NCPI is tested in the following several probable operating conditions:

A. Voltage stability analysis

In this part, the maximum load-abilities for the weak buses and critical lines are identified. The maximum allowable loads in each specific bus have been ranked in ascending order to identify the weak area in the system. The performance of *NCPI* is tested on two IEEE test systems to validate its practicability in the following cases:

- Base load
- Heavy active power load
- Heavy reactive power load
- Heavy apparent power load

B. Contingency ranking and analysis

NCPI is tested during several contingencies to examine its capability and determine the most sensitive line in the system due to line or generator outages, as in the following cases:

- Base load with line outage contingency (N-1)
- Predetermined reactive power load with line outage contingency (N-1)
- Predetermined reactive power load with two lines outage contingencies (N-2)
- Predetermined reactive power load with generator outage contingency (N-1)
- Predetermined reactive power load with two generators outage contingencies (N-2)

3. For verification purposes, the proposed *NCPI* index is compared with the well-known line voltage stability indices (L_{mn}, *FVSI*, *LQP*, *NLSI* and *VSLI*) in different operating scenarios in the system. All the line voltage stability indices are based on the same theoretical foundations, and the difference is only in the assumptions used in each index [36–38]. Therefore, some sensitive assumptions should be considered to predict voltage collapse accurately. The sensitive assumptions that affect the accuracy of the voltage collapse prediction are explained in Sect. 3.3.
4. *NCPI* is proposed to predict the voltage collapse events and risks of loading stress in the lines. Unlike the above existing indices, the proposed method

takes into account all the sensitive assumptions that affect the accurate diagnosis of the collapse problem to accurately predict the voltage instability. Therefore, the proposed index gives more accurate results than the other stability indices (more details are given in Sect. 3.3).

5. This study provides general guidelines for researchers to avoid the sensitive assumptions that affect the precise diagnosis of voltage collapse. It also aims to select an appropriate index that can adapt to several operating scenarios and with several electric power networks. Selecting a suitable stability index that accurately identifies the critical line during actual operation is important. In many cases, the other indices diagnose many critical lines as healthy lines, while interrupting a line from the system may cause successive line interruptions and an entire system blackout. The uniqueness of the proposed *NCPI* index is that it can accurately predict voltage collapse under several operating loadings and contingencies.

6. The proposed index has a predictable shape since it has a high response due to any variation events. This characteristic can help the operators smoothly determine how far the system is from collapse and subsequently make rectifications in time. In contrast, it is very hard for the operators to make corrections in time when the index fails to determine the voltage collapse points.

Subsequent discussion and analysis are organized and coordinated as follows: Sect. 2 presents the existing voltage stability indices and their limitations, while Sect. 3 presents the formulation of the proposed index *NCPI*, considerations of its calculation and the sensitive assumptions of the existing indices. Section 4 shows the voltage stability analysis based on *NCPI*, while Sect. 5 presents the contingency ranking and analysis based on *NCPI*. Case studies and simulation results are shown in Sect. 6, and the conclusion is presented in Sect. 7.

2 Voltage stability indices (VSIs) and their limitations

VSIs are used as measurement tools to determine whether a system is stable or not, and how close a system is to the points of instability. There are many methods for voltage stability assessment that have been suggested in the literature. In [36], three categories of VSIs are classified: line VSIs, bus VSIs, and overall VSIs. The classification of VSIs, as illustrated in [38], can be grouped into four types: (1) line variables based-indices; (2) bus variables based-indices; (3) Jacobian matrix-based indices; and (4) Phasor Measurement Units (PMU)-based indices. Jacobian matrix-based indices can identify the

voltage collapse points and determine the stability margin. However, these indices require a long computation time since the Jacobian matrix changes with any topological changes, and the matrix must be recalculated. Therefore, they are inappropriate for real-time voltage stability assessment. Moreover, Jacobian matrix based-indices increase the running time of the optimization problem, especially in a large power system [36–38, 65]. Hence, these indices require more computation effort, and the cost of calculation will be very high.

The PV and QV curves that are developed by conventional power flow can be used to determine the stability margin but they must be generated at each bus [72]. In addition, they require information about the power system beyond the operating points. Hence, the calculation cost is also very high. In contrast, line and bus voltage stability indices require less computation since they are based on system variables and are sufficient for real-time application [36].

Bus VSIs determine the voltage stability of system buses but they do not provide any information about the weak facilities and the probability of voltage instability in the system [36–38]. Line voltage stability indices (LVSIs) are the simplest indices that are appropriate instruments to determine the power system's weak buses and critical lines, and are suitable for evaluating voltage stability for lines and buses. In addition, they are suitable for solving optimization problems because of their ability to determine weak areas in the power systems [51, 73].

Line voltage stability indices (LVSIs) can be used online and/or offline [36, 45, 74–78]. LVSIs are used as instruments that can monitor the value of LVSIs and take suitable corrections in time when the values of the indices approach the stability limit. These indicators are used as measurement tools that are noticed because of any change in the system parameters.

LVSIs should have a predictable shape and high performance with system variations relating to voltage instability. They should also be simple, convenient for application and computationally efficient. It is critical to have precise knowledge to determine how close an operating system is to the threshold level of voltage stability [79–81]. It has been noted that the voltage magnitudes alone may not appear to be a good indicator of approaching a threshold level of voltage stability. Hence, VSIs should give trustworthy details on the closeness of voltage instability and highlight the robustness of a power system to resist load increases or outages.

2.1 Line voltage stability index (L_{mn})

L_{mn} indicator is proposed in [66], which uses the concept of power transfer between two nodes of a single transmission line, given as:

$$L_{mn} = \frac{4XQ_j}{(V_s \sin(\theta - \delta))^2} \le 1 \qquad (1)$$

The defect of this index is that it fails to predict collapse during very high active or apparent power loading because it ignores the active power effect. It also ignores the effect of the shunt admittance.

2.2 Fast voltage stability index (*FVSI*)
Use *FVSI* is proposed in [67] by simplifying the L_{ij} index [82]. The occurrence of voltage collapse during a contingency scenario is used to calculate this index. The formulation below shows that the *FVSI* index is a simplified L_{mn} equation form by ignoring the voltage angle difference between the sending and receiving buses, i.e., $\delta = 0$, as:

$$FVSI = \frac{4Z^2 Q_j}{V_i^2 X} \le 1 \qquad (2)$$

When the angle difference is considered to be zero ($\delta = 0$), L_{mn} in (1) becomes:

$$L_{mn} = \frac{4XQ_j}{V_i^2 \sin^2(\theta)} \le 1 \qquad (3)$$

Recalling the line impedance from the equation $X = Z \sin(\theta)$ yields:

$$\sin(\theta) = \frac{X}{Z} \qquad (4)$$

By replacing (4) in (3), the index is:

$$FVSI = L_{mn} = \frac{4Z^2 Q_j}{V_i^2 X} \le 1 \qquad (5)$$

The active power variations, shunt admittances and angle differences are all ignored. Hence this index is a low time-consuming calculation but is inaccurate because it ignores the active power variations and angle differences. The rising angle disparities between West Michigan and Cleveland created the blackout of the Northeastern Area, according to Ian Dobson et al. [83], demonstrating that significant angle changes represent a risk signal for the development of cascading outages and/or network blackouts.

2.3 Line stability factor (*LQP*)
Reference [68] uses the power-flow (PF) theory on a single power transmission line to formulate the line stability factor (*LQP*). The resistances of lines are ignored to simplify the index, i.e., the lines are considered as lossless lines ($P_i = P_j$). Also, this index doesn't consider the relative direction of power flow. *LQP* is derived as:

$$LQP = 4\left(\frac{X}{V_i^2}\right)\left(\frac{P_i^2 X}{V_i^2} + Q_j\right) \le 1 \qquad (6)$$

The system is said to be stable when the *LQP* value is less than unity.

2.4 Novel line stability index (*NLSI*)
Based on the same principle as L_P in [84], reference [69] develops a line stability index. The angular difference between the sending and receiving end voltages is assumed to be very small (zero) in this index, and the shunt admittance of the line is ignored. This index is formulated as:

$$NLSI = \frac{P_j R + Q_j X}{0.25 V_i^2} \le 1 \qquad (7)$$

The active and reactive power are related to the *NLSI* index, as shown in (7). However, *NLSI* also doesn't consider the relative directions of power flow.

2.5 Voltage stability load index (*VSLI*)
VSLI is proposed in [71] for assessing line voltage stability based on the same idea of L_P [84], as:

$$VSLI = 4\frac{[V_i V_j \cos(\delta) - V_j^2 \cos^2(\delta)]}{V_i^2} \le 1 \qquad (8)$$

VSLI can be computed for real-time monitoring using PMU measurements of sending and receiving voltage magnitudes and the angle difference. As with all prior indices, the shunt admittances of lines are ignored in this index. The *VSLI* value must be lower than 1.00 to keep the system stable.

3 Proposed novel collapse prediction index *NCPI*
3.1 Formulation of the proposed index *NCPI*
The formulation of the index *LQP* is based on entirely ignoring the line resistance. This leads to erroneous collapse predictions. This index also ignores the relative direction of active power flow in a line in relation to reactive power flow. In order to avoid these drawbacks, an improved Novel Collapse Prediction Index (*NCPI*) is formulated based on partially ignoring the resistance of a transmission line, while taking into account the impacts of the active and reactive power flow on the system voltage stability.

NCPI is developed for electrical power systems to monitor voltage stability circumstances or to predict voltage instability. A simplified model of an electric power transmission system from bus-i to bus-j through a transfer branch with a branch impedance ($Z = R + jX$) is shown in Fig. 1. V_i and V_j depict the sending and receiving voltages,
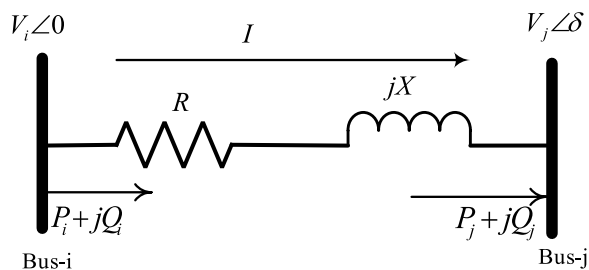
Fig. 1 Single line diagram of power transmission line

respectively. The angle (δ) represents the voltage angle difference between the sending voltage angle (δ_i) and the receiving voltage angle (δ_j). The sending voltage is taken as a reference so its angle is zero. P_i and Q_i illustrate the active and reactive power at the sending end, while P_j and Q_j depict the active and reactive power at the receiving end, respectively. Z, R and X represent the impedance, resistance and inductance of a line, respectively.

The transmission line current flowing between bus-i and bus-j can be represented as:

$$I = \frac{V_i \angle 0 - V_j \angle \delta}{R + jX} \tag{9}$$

The complex apparent power at bus-j can be represented as:

$$S_j = V_j I^* \tag{10}$$

Rearranging (10), the line current can be rewritten as:

$$I = \left(\frac{S_j}{V_j}\right)^* = \frac{P_j - jQ_j}{V_j \angle -\delta} \tag{11}$$

Replacing the line current in (11) by (9) yields:

$$\frac{V_i \angle 0 - V_j \angle \delta}{R + jX} = \frac{P_j - jQ_j}{V_j \angle -\delta} \tag{12}$$

$$V_i V_j \angle -\delta - V_j^2 \angle 0 = (R + jX)(P_j - jQ_j) \tag{13}$$

$$V_i V_j \cos\delta - V_j^2 = RP_j + XQ_j \tag{14}$$

$$-V_i V_j \sin\delta = XP_j + RQ_j \tag{15}$$

Reorganizing (15) for P_j and Q_j, and substituting into (14) yield the equations of active and reactive power at the receiving end as:

$$P_j = \left[(V_i \cos(\delta) - V_j)R - V_i X \sin(\delta)\right]\frac{V_j}{R^2 + X^2} \tag{16}$$

$$Q_j = \left[(V_i \cos(\delta) - V_j)X + (V_i \sin(\delta))R\right]\frac{V_j}{R^2 + X^2} \tag{17}$$

where $Z^2 = R^2 + X^2$.

In [68, 70], the resistance of the line is ignored in (16) and (17). The new hypothesis in this paper is that the line resistance is only partially ignored because entirely ignoring the line resistance, such as in *LQP*, results in an enormous error in voltage instability prediction and generates a high difference in the stability index value. For instance, the critical line may be identified as a healthy line by ignoring the line resistances. The meticulous investigation and comparison of the results when the resistances of branches are entirely and partially ignored are used to evaluate the instability prediction. The terms $(V_i \cos(\delta) - V_j)R$ in (16) and $(V_i \sin(\delta))R$ in (17) are very small since they are multiplied by the line resistance. The terms $(V_i \cos(\delta) - V_j)R$ in (16) and $(V_i \sin(\delta))R$ in (17) are negligible and taken as zero to simplify (16) and (17).

Equations (16) and (17) are simplified to:

$$P_j = \frac{X}{Z^2}(-V_i V_j \sin(\delta)) \tag{18}$$

$$Q_j = \frac{X}{Z^2}(V_i V_j \cos(\delta) - V_j^2) \tag{19}$$

where $Z^2 = R^2 + X^2$.

The line resistance is considered in the square term of line impedance ($Z^2 = R^2 + X^2$) to guarantee the accuracy of the prediction index. The impedance square is taken into account to avoid equally putting the reactance value with the impedance value, i.e., $Z^2 \neq X^2$. These terms have high sensitivity in the collapse prediction and affect the other parameters and variables when line resistances are ignored. It means that the term X/Z^2 in (18) and (19) yields $1/X$ if the line resistance is further ignored, i.e., $Z = X$. In order to prevent abbreviating the line reactance in the numerator with the line impedance in the denominator, which would significantly affect index accuracy, the square of the line impedance is considered. This technique takes into account the square of the line impedance to obtain a more accurate stability index since considering line impedance does not affect the processing of simplifying equations and will support the index value. Hence, the technique depends on neglecting the resistance of a portion but not entirely of the system to formulate an approximate and rapid collapse prediction index.

By rearranging (18) and (19) and taking out δ by using $\sin^2(\delta) + \cos^2(\delta) = 1$, a second-order formula of the quadratic voltage equation can be depicted as:

$$V_j^4 + V_j^2 \left(\frac{2Q_j Z^2}{X} - V_i^2 \right) + \frac{Z^4(P_j^2 + Q_j^2)}{X^2} = 0 \quad (20)$$

To preserve voltage stability, the discriminant of (20) must be greater than or equal to zero. The state to have at least a solution is:

$$\left(\frac{2Q_j Z^2}{X} - V_i^2 \right)^2 - 4\frac{Z^4(P_j^2 + Q_j^2)}{X^2} \geq 0 \quad (21)$$

Equation (21) can be further expanded as:

$$\frac{4Z^4 Q_j^2}{X^2} - \frac{4Q_j Z^2}{X} V_i^2 + V_i^4 - 4\frac{Z^4 P_j^2}{X^2} - 4\frac{Z^4 Q_j^2}{X^2} \geq 0 \quad (22)$$

Equation (22) can then be simplified as:

$$V_i^4 - \frac{4Q_j Z^2}{X} V_i^2 - 4\frac{Z^4 P_j^2}{X^2} \geq 0 \quad (23)$$

The novel collapse prediction index (*NCPI*) is thus given as:

$$NCPI = \frac{4Z^2}{XV_i^2} \left(\frac{Z^2 P_j^2}{XV_i^2} + |Q_j| \right) \leq 1 \quad (24)$$

It is observed that the second part of (24) represents the index *FVSI* in (2), so (24) can be rewritten as:

$$NCPI = \frac{4Z^4 P_j^2}{X^2 V_i^4} + FVSI \leq 1. \quad (25)$$

3.2 Considerations for the proposed index *NCPI*
The index *NCPI* takes into account the magnitude of reactive power at the receiving end and the relative directions of active and reactive power flow because of the following technical reasons:

- Logically, as the load increases, the stability indices progressively increase until the power flow fails to provide a solution. At the voltage collapse point, the indices should become closer or equal to the stability limit (unity). From (24), it is seen that the first and second terms of the equation will be subtracted while the sign of the receiving reactive power is negative. This causes a decrease in the index value. The effect on the index value will be significant in the case of heavy active and reactive power (heavy apparent power) when the sign of the reactive power is negative, even if the load reaches the critical level.
- The magnitude of the line impedance square is expressed as $Z^2 = R^2 + X^2$. Therefore, the RP_j in the

first term of (24) represents the resistive voltage drop created by active power, while XQ_j in the second term represents the inductance voltage drop produced by the reactive power of a line. The sign of active power at the receiving end remains positive since its parameter is in a quadratic form. Therefore, the voltage drop of the second term of the equation will be subtracted from the first term while the sign of receiving reactive power is negative, and this causes a decrease in the index value.

- From (24), it is noted that the second term of the equation represents the index *FVSI* as simplified in (25). Therefore, during the same power flow direction, the value of the proposed index *NCPI* will be lower than *FVSI*, and this scenario is the opposite of the proposed index target. The proposed index aims to improve the index value by adding the active power variation to identify the voltage collapse accurately.

3.3 Sensitivity assumptions and expected results theoretically for all LVSIs
There are some sensitivity assumptions that must be considered in the existing stability indices. The main drawback of *FVSI* is that the index gives an incorrect collapse prediction when active power is high since it ignores the effect of active power flow [41]. The index *FVSI* has high performance during heavy reactive power since it strongly relates to reactive power flow. Hence, this paper proposes *NCPI* as a new collapse prediction index. This strongly relates to active and reactive power at the receiving bus, as illustrated in (24).

Therefore, the proposed index can predict collapse due to either active, reactive, or apparent power variations. From (25), the *NCPI* values are expected to be almost consistent with the *FVSI* values during heavy reactive power variations. In order to determine the maximum reactive power load-ability, the reactive power gradually increases till the indices approach the stability limit or the power flow doesn't converge. Conversely, the active power stays constant at the base load. Hence, its value is small compared to the maximum reactive power load. The values of *NCPI* and *FVSI* are almost the same for these logical and technical reasons. The value of *FVSI* will be low because of heavy active power variation since *FVSI* ignores the effect of active power. In contrast, the proposed index *NCPI* will have a high response in collapse prediction since it relates to the square of the active power, as shown in (24). When active and reactive power variations in the system occur, *FVSI* only has a response with half the variation (reactive power variation). Hence, *FVSI* also has low performance in collapse prediction

for this condition. Conversely, the proposed index *NCPI* will have a high performance since it relates to active and reactive power variations.

L_{mn} is similar to *FVSI*, where the L_{mn} also ignores the effect of active power. *FVSI* is a simplified equation of L_{mn} when the voltage angle difference is ignored, as shown in (5). In a few cases, L_{mn} has high performance in collapse prediction with active power since the index indirectly relates to active power through the voltage angle difference, as shown in (1).

The index *NLSI* has low performance in heavy active power since the index ignores the voltage angle difference, which is high because of heavy active power. In some cases, the index *NLSI* reaches a stressed level because of heavy reactive power. *NLSI* ignores the relative directions of active and reactive power flow. From (7), the value of *NLSI* will be high when the active and reactive power flow in the same direction. Conversely, the value of *NLSI* will be very low when the active and reactive power flow in the opposite direction, so the critical lines are detected as healthy lines in this condition. This is because the first and second terms of (7) are subtracted, resulting in reducing the *NLSI* value. For this reason, *NLSI* fails to determine the voltage collapse in most cases during heavy apparent power.

The index *LQP* has many sensitivity assumptions. *LQP* supposes the sending and receiving power are equal (lossless line), which leads to the fact that *LQP* surpasses the stability limit in some cases during heavy active power at the maximum loading. Similarly, *LQP* entirely ignores the line resistance, which results in an enormous error in collapse prediction when the line resistance is high. Because of this, the index *LQP* has a weak response during heavy reactive power. The index *LQP* fails to identify the voltage collapse during heavy apparent power load except for a few cases since it doesn't consider the relative directions of active and reactive power flow. From (6), it is seen that the active power is in quadratic form. The first and second terms are subtracted when the power flow is in the same direction. Hence, the index *LQP* fails to identify voltage collapse in this condition, and the index value will be very low. The index *LQP* will have a high value when the active and reactive power are in the opposite directions. Nevertheless, the index still gives inaccurate results since the resistance is entirely ignored.

VSLI has high performance during heavy active and apparent power loads. Nevertheless, *VSLI* fails to approach the stability limit in some cases. From (8), it can be seen that *VSLI* is not directly related to active and reactive power, whereas the proposed index is.

The proposed index *NCPI* considers all the sensitive assumptions mentioned above to identify the collapse accurately. *NCPI* takes into account the effect of active

and reactive power and their relative directions. *NCPI* also doesn't ignore the voltage angle difference. From (24), it is observed that *NCPI* has a relationship with the line impedance since the line resistance is not entirely ignored. As a result, *NCPI* is a unique index with high accuracy for predicting voltage collapse and/or monitoring crucial lines and weak buses in power systems. The suggested index is precise, efficient, rapid, and simple. *NCPI* is rapid for instability prediction since its equation is short and depends on five variables and parameters (P_j, Q_j, Z, X and V_i), as shown in (24). For a system to be stable, the *NCPI* value must be less than one; otherwise, collapse imminent.

3.4 Advantages of the proposed index *NCPI*

The proposed index has multiple advantages for an electrical power system:

(1) The proposed index *NCPI* can be adapted to different power operating scenarios. It has high performance in collapse prediction during any sudden variations in the system, including active power, reactive power, or both active and reactive power. It is a unique property in the proposed index since the other voltage stability indices are unable to adapt to different power operating scenarios.

(2) It can be used to estimate the maximum load-ability and identification of weak buses and critical lines. Therefore, the weak areas of the system can be determined and supported by the following countermeasures:

- At the planning stage of the power system, weak buses and lines can be supported by distributed generation units or other voltage-supporting equipment.
- Shunt capacitor switching or load shedding.
- Flexible AC transmission line system (FACTS) to enhance the voltage stability margin.
- Tap changer switching.

The case studies determine the weak areas that required support by suitable countermeasures mentioned above.

(3) *NCPI* provides the operators with accurate information about the system stability during operation. This is because the proposed index has a high performance with several power system operations. Therefore, the index *NCPI* has a predictable shape. Its value varies between zero and the stability limit (1.00) in a semi-linear curve with high response because of power variations. The operators can

smoothly monitor the system using the *NCPI* instrument and make corrections in time to avoid voltage collapse.

(4) The proposed index is an effective instrument in contingency ranking and analysis since it can provide a priori prediction of the most critical and stressed lines because of line or generator outage contingency. Therefore, the operators can identify the most critical and/or sensitive lines that need suitable control action because of the generator or line outage contingency.

(5) LVSIs can be incorporated into the conventional optimum power flow (OPF) to enhance the voltage stability margin and reduce power loss [56]. Therefore, *NCPI* is an effective index for improving the stability margin since it is effective over several operating conditions.

4 Voltage stability analysis based on *NCPI*

The main goal of voltage stability analysis is to determine the voltage collapse points, maximum load-ability, weak buses and critical lines using the proposed index *NCPI*. Voltage stability normally has a high sensitivity to reactive power load. Therefore, the heavy reactive power at each particular bus is determined to identify the weak buses and critical lines. The performance of *NCPI* is investigated to determine maximum load-ability, weak buses and critical lines, using the following procedure:

1. Input the data of the electric power system.
2. The Newton Raphson (NR) method is used to run the power flow solution in the base case loading.
3. The proposed *NCPI* values are calculated for normal loading.
4. The maximum allowable reactive power load of each particular bus is determined by increasing the load by a specific amount gradually till there is a divergence of power flow or the index value approaches the stability limit (1.00).
5. The solution doesn't converge when the load exceeds the limit. In this case, shedding the load by a specific amount to determine the voltage collapse point.
6. For each load increase, the *NCPI* gradually increases from zero to the stability limit.
7. Determine the lines with the highest stability index values. This denotes that those lines are the most critical.
8. Select another load bus and repeat steps 1–7.
9. The maximum load-ability for each selected bus can be smoothly determined from step 4.

10. Sort the maximum load-ability in ascending order from step 9. The bus with the minimum allowable load is ranked first, indicating that it is the weakest bus in the system.
11. Repeat the previous steps for verification using the well-known stability indices (L_{mn}, *FVSI*, *LQP*, *NLSI*, and *VSLI*).
12. Compare the performance of the *NCPI* with that of existing indices.
13. Because of space restrictions, heavy active and reactive power loads are applied to some load buses from different areas in the system to investigate the performance of the proposed index in different probable operating conditions.

The flowchart in Fig. 2 shows the whole procedure for weak buses and critical line identification. The closeness of the *NCPI* value to 1.00 determines the critical lines referred to a specific bus and voltage stability conditions. The active and reactive power changes are more probable components in a practical power system. While the indices L_{mn} [66], *FVSI* [67], *LQP* [68], *NLSI* [69] and *VSLI* [71] do not take into account these critical variations, the proposed index *NCPI* considers all the probable operating scenarios in the two IEEE test systems.
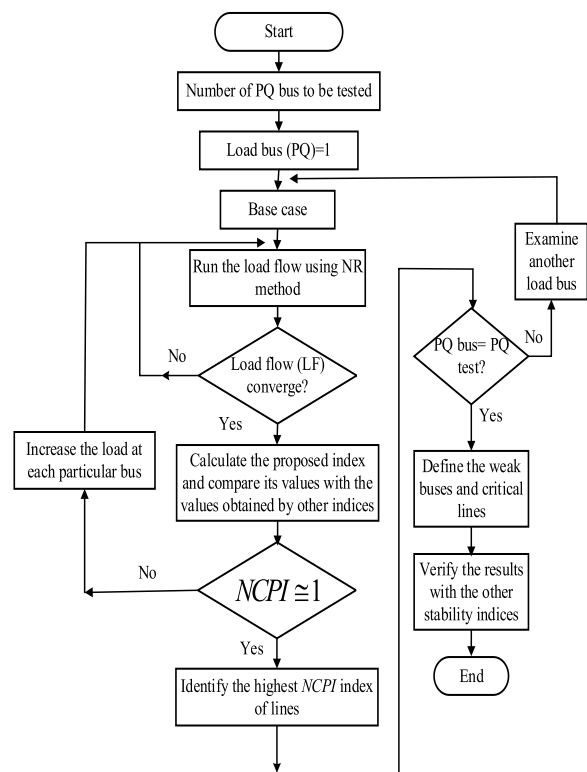

Fig. 2 Flow chart for weak buses and critical lines identification

5 Contingency ranking and analysis based on *NCPI*

Contingency is one of the contributing reasons for voltage violations in a power system. The procedure of contingency ranking and analysis is illustrated in Fig. 3. Line outages contingency (LOC), and generator outages contingency (GOC) can occur as a single (N-1) or series outage (N-multiple outages).

To assess the effectiveness of the *NCPI* in predicting voltage collapse during line or generator outage, contingency analysis is carried out under the base load as well as predetermined load as illustrated in the following:

1. Run the power flow with a line or generator outage contingency during a base case loading.
2. Calculate the proposed index values for all the lines.
3. Rank the lines based on the proposed index in descending order. The lines with the highest values of the proposed index are considered the most sensitive. If the index values of these lines approach unity, the lines are considered the most critical lines in the system. The system is said to be unsta-

ble if the load doesn't converge or the index values reach the stability limit.
4. Insert back the outage generator or line.
5. Examine another line or generator outage and repeat steps 1–4.
6. Predetermined reactive power (half of the maximum load-ability) is applied to the selected test system and then the power flow is run.
7. Repeat steps 2–4 for the predetermined load condition.
8. Examine another load bus (PQ bus).
9. Verify the results with other existing indices.
10. List the contingency ranking for each case.

As a result, the contingency ranking due to the severity of the line outage or generator outage is constructed. The results show the most sensitive or critical line due to line outage or generation unit outage, which has the highest *NCPI* value among the lines. The most critical line is eligible to be interrupted from the service due to a line outage. In this case, a series of line outages will occur if operators don't make rectifications in time.

6 Case studies and simulation results

The IEEE 30-bus and IEEE 118-bus systems [85] are used to investigate the practicability of the suggested index. In order to examine the feasibility of the proposed index, the implementation results are analyzed and compared with other most important indices. To determine overall system performance, the studies in each test system are implemented for several criteria based on the loading components and contingencies. The IEEE 30-bus and IEEE 118-bus test systems are examined during several power load conditions and contingencies to prove the practicability of the suggested index. The line diagrams of the IEEE 30-bus and IEEE 118-bus are shown in Figs. 4 and 5, respectively.

6.1 Voltage stability analysis
6.1.1 IEEE 30-bus test system
The IEEE 30-bus system contains 24 load buses, six generator buses, and 41 branches [85]. The system is examined during several operating load conditions.

6.1.1.1 Base case loading The loads at the base load condition are constant at all the load buses. Other widely adopted voltage stability indices are computed and compared with the *NCPI*, as shown in Table 1. The proximity of the proposed index to 1.00 denotes the stressed condition of a line, and when the line is secure, the proposed index is less than the stability limit (1.00).

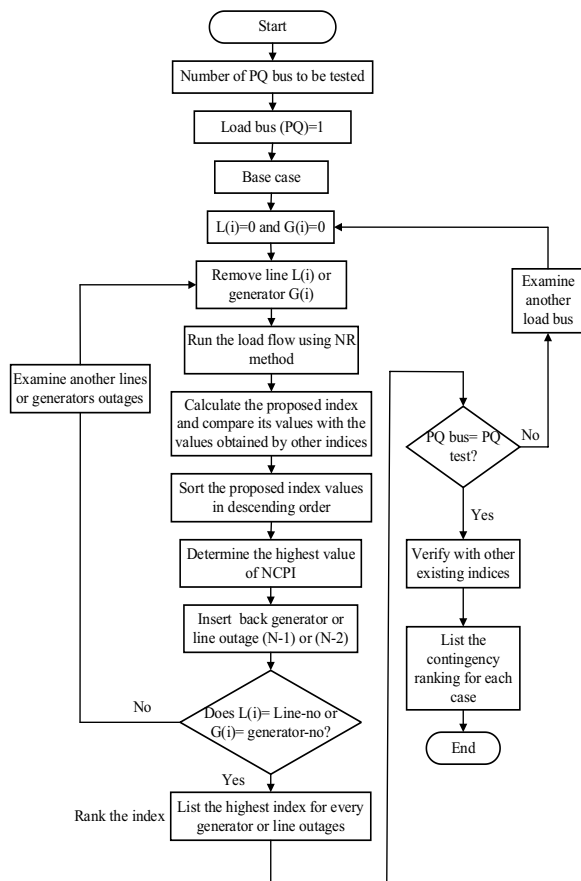Table 1 shows that the proposed index in each case offers values slightly higher than the values of L_{mn}, FVSI

Fig. 3 Flow chart for contingency ranking and analysis
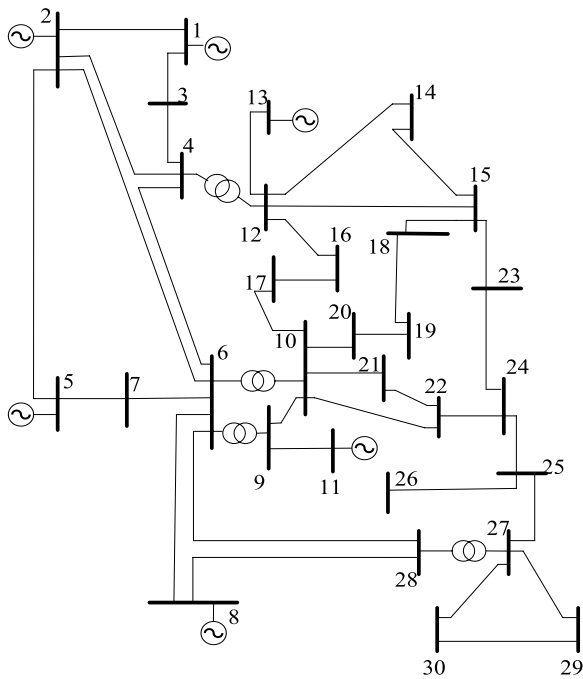
Fig. 4 Line diagram of the IEEE 30-bus test system

and *LQP*. This is because the proposed index doesn't entirely ignore the line resistance and considers the magnitude of reactive power and the directions of power flow. As a result, when the signs of active and reactive power are negative (same direction), the voltage drop due to the resistance subtracts the voltage drop due to the reactance, which makes the index value low. The proposed index considers the magnitude of reactive power to avoid this dilemma, whereas the other indices do not consider the influence of power flow directions. The indices *NLSI* and *VSLI* offer different values in comparison to the other stability indices. The proposed index values are sometimes higher than the values of *NLSI* and *VSLI* and vice versa. In contrast, the proposed index *NCPI*, L_{mn} and *FVSI* are almost consistent in most cases.

The index *LQP* offers values slightly lower than *NCPI*, L_{mn}, and *FVSI* since the index *LQP* entirely ignores line resistance. It can also be noticed that the values of the proposed index are consistent with the other indices for line 9–11 since the resistance of this line is zero. As a result, the proposed index offers a precise instrument for estimating voltage stability. The system is stable since the values of all stability indices approach zero.

Fig. 5 Line diagram of the IEEE 118-bus test system

Table 1 The line stability indices for the IEEE 30-bus system in the base case loading

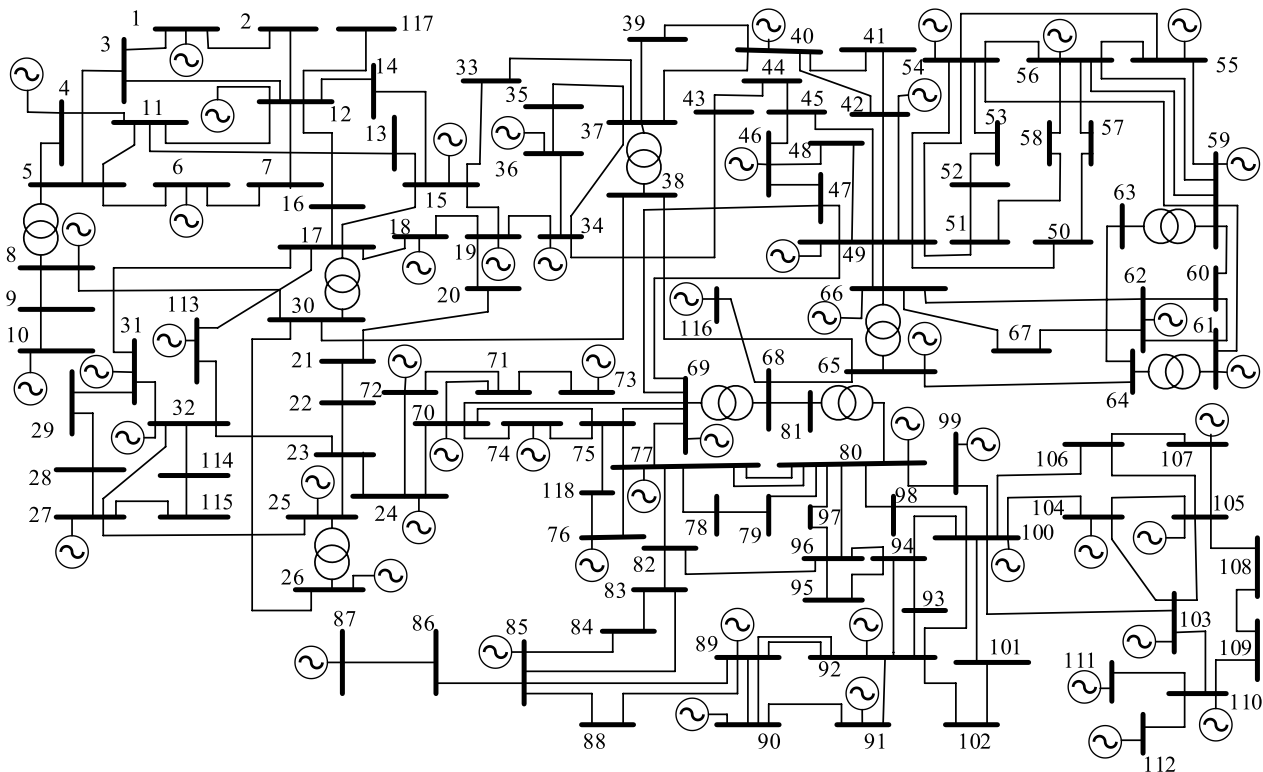| Line	NCPI	L_{mn}	FVSI	LQP	NLSI	VSLI
6–4	0.0364	0.0333	0.0326	0.0334	0.0021	0.0049
6–28	0.0249	0.0242	0.0243	0.0221	0.0101	0.0049
9–11	0.1113	0.1113	0.1113	0.1113	0.1113	0.1113
16–17	0.0121	0.0119	0.0118	0.0098	0.0210	0.0211
18–15	0.0177	0.0169	0.0167	0.0129	0.0373	0.0377
20–10	0.0328	0.0315	0.0310	0.0247	0.0566	0.0574
21–10	0.0328	0.0323	0.0321	0.0259	0.0463	0.0465
25–24	0.0267	0.0263	0.0266	0.0199	0.0104	0.0106
24–23	0.0164	0.0162	0.0162	0.0130	0.0219	0.0219
30–27	0.0502	0.0415	0.0398	0.0245	0.1154	0.1205
30–29	0.0142	0.0126	0.0124	0.0086	0.0445	0.0454

Table 2 Heavy active power at some load buses of the IEEE 30-bus test system

Bus no.	Active power (MW)	Most critical lines	Lines (from–to)	NCPI	L_{mn}	FVSI	LQP	NLSI	VSLI
Bus-4	618	4–2	4–2	1.0047	0.8524	0.3518	1.3020	0.2089	0.9335
			4–3	0.5587	0.5771	0.4670	0.5783	0.1575	0.0392
			4–12	0.4541	0.43034	0.4264	0.3987	0.4264	0.5848
			4–6	0.4169	0.4027	0.3867	0.3277	0.4495	0.4608
Bus-7	513	7–6	7–6	1.0203	0.9545	0.4054	1.1558	0.1592	0.9090
			7–5	0.7753	0.7013	0.5258	0.1669	0.7967	0.9115
Bus-14	137.8	14–15	14–15	0.9951	0.8172	0.3127	0.3941	0.6593	0.8521
			14–12	0.6571	0.3830	0.2147	0.3175	0.6940	0.8422
Bus-19	133.5	1–3	1–3	0.9201	0.5455	0.4957	0.7872	0.7265	0.5499
			18–15	0.4935	0.2237	0.1710	0.0507	0.5110	0.6309
Bus-28	486.01	28–6	28–6	0.9403	0.3756	0.2598	0.9056	0.2541	0.7882
			28–8	0.8334	0.6952	0.5102	0.1301	0.7673	0.8240
			28–27	0.1974	0.1830	0.1724	0.1974	0.1824	0.2090

6.1.1.2 Heavy active power loading   As shown in Table 2, at each selected load bus, the active power loading is gradually increased until the voltage collapse points to investigate the effect of heavy active power loading on the proposed index *NCPI*. When the active power at each load bus increases to the maximum allowable value, the proposed index increases to unity, as shown in Table 2. Conversely, the L_{mn}, *FVSI*, *LQP* and *NLSI* are far from the critical level (1.00), which indicates that these indices fail to detect the voltage collapse points. It is observed that the index *VSLI* reaches the stability limit in most cases. However, *VSLI* fails to detect the collapse for branches 1–3 and 28–6 because of heavy active power at buses 19 and 28.

L_{mn} and *FVSI* have low response since they ignore the effect of active power flow. The values of L_{mn} and *FVSI* indicate that ignoring the active power effect creates erroneous collapse prediction where the critical lines have been diagnosed as healthy lines. L_{mn} diagnoses only branch 7–6

as the critical line since the index is indirectly related to the active power through the voltage angle difference, while it diagnoses all the remaining branches as healthy lines.

The index *NLSI* ignores the voltage angle difference and relative directions of active and reactive power flow. Therefore, the results of *NLSI* show an inadequate response in this case, and the values are too far from the stability limit (unity).

It can be seen that the index *LQP* increases to 1.302 and 1.1558 for branches 4–2 and 7–6. These values denote that the collapse had already occurred. It is expected since the index supposes the lines to be lossless ($P_i = P_j$). The *LQP* index reaches 0.3941 and 0.7872 for branches 14–15 and 1–3, respectively, since *LQP* entirely ignores line resistance and doesn't consider the relative directions of active and reactive power flow.

As a result, the other indices show erroneous states of voltage stability. Figure 6 shows the variations of voltage
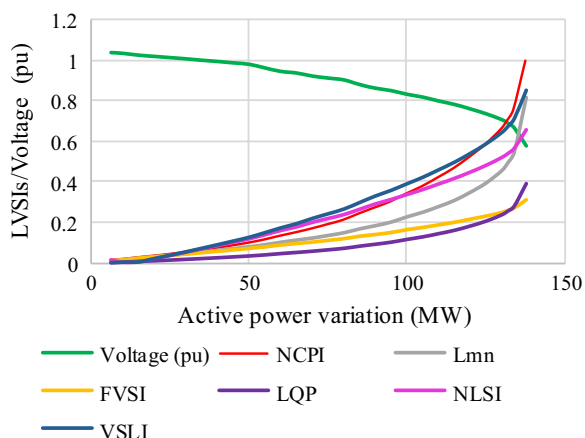
Fig. 6 Variations of line voltage stability indices (LVSIs) for branch 14–15 during active power variations at bus 14

stability indices for branch 14–15 during active power variation at bus 14. It is noted that the performance of *NCPI* is better than other indices. *NCPI* reaches 0.72, which is higher than other index values when the power reaches 132 MW. In this case, *NCPI* informs the operator that the voltage collapse is close to occurring to rectify the system in time. If the operator doesn't make rectification in time, *NCPI* will increase further because of the increase in active power, and the collapse will occur when the active power reaches 137.8 MW.

6.1.1.3 Heavy reactive power loading The effectiveness and practicability of the suggested index are examined under heavy reactive loading by gradually increasing the reactive power loading on each bus until the loading reaches the voltage collapse point. Consequently, the proposed index *NCPI* gradually increases until it approaches the stability limit (1.00). *NCPI* is calculated and compared with the other indices, and the results are shown in Table 3. The maximum reactive power load-abilities have been determined to identify the weak buses of the system. The reactive power load is considered a maximum allowable reactive power load when the index reaches the stability limit. Any addition of load beyond this level makes the solution of power flow non-converging. The application results of only some buses are presented in the table because of space restrictions. It can be seen that the proposed index *NCPI* is the closest index to 1.00 among voltage stability indices in each specific load bus because of heavy reactive loading. It is noted that L_{mn} and *FVSI* have high response in this condition.

The *LQP* index offers lower values and shows the weakest performance among all the indices because of heavy reactive power loading. It can be seen that the *LQP* index diagnoses the critical lines as healthy lines in most cases. It is seen that the proposed index values for branches 26–25 and 30–27 approach unity. *FVSI* verifies the value of the proposed index for branch 26–25, while L_{mn}, *FVSI*, *NLSI* and *VSLI* verify the value of the proposed index for branch 30–27. However, *LQP* diagnoses these branches as healthy lines. This deceptive prediction is repeated for branches 14–15 and 24–22, where *LQP* increases to 0.4405 and 0.6932 at the maximum reactive power load. This is because the resistances of these branches are

Table 3 Heavy reactive power at some load buses of the IEEE 30-bus test system

Bus no.	Reactive power (MVAr)	Most critical lines	Lines (from–to)	NCPI	L_{mn}	FVSI	LQP	NLSI	VSLI
Bus-26	31.5	26–25	26–25	1.0086	0.8633	1.0055	0.6814	0.7459	0.7835
Bus-30	34.15	30–27	30–27	1.0091	0.9726	1.0038	0.7384	0.9528	0.9593
			30–29	0.8119	0.7822	0.8025	0.6244	0.7394	0.7459
Bus-14	96.5	14–15	14–15	1.0018	0.7776	0.9943	0.4405	0.5328	0.5763
			14–12	0.8540	0.7786	0.8540	0.6915	0.6891	0.7185
Bus-24	114	24–22	24–22	1.0020	0.8666	0.9986	0.6932	0.7597	0.7943
			24–23	0.8101	0.7478	0.8097	0.6500	0.6697	0.6902
			24–25	0.7517	0.6815	0.7517	0.5646	0.5715	0.5962
Bus-9	291.5	9–11	9–11	0.9807	0.9807	0.9807	0.9807	0.9807	0.9807
			9–6	0.9786	0.9757	0.9719	0.9651	0.9719	0.9206
			9–10	0.5930	0.5892	0.5881	0.5832	0.5881	0.5930
Bus-28	364	28–8	28–8	0.9981	0.9350	0.9917	0.8962	0.8957	0.9108
			28–6	0.8575	0.8314	0.8569	0.7893	0.8072	0.8067
			28–27	0.3405	0.3004	0.2964	0.2523	0.2964	0.4313
Bus-3	410	3–1	3–1	0.9994	0.9964	0.9435	0.7943	0.9913	0.9967
			3–4	0.8595	0.7877	0.8508	0.7573	0.7008	0.7468

high, as shown in [85]. It is noted that the *LQP* index is near1.00 for branch 28–8 since the line resistance of branch 28–8 is low, while the *LQP* index is close to unity when the line resistance is zero, such as line 9–11.

NLSI and *VSLI*, in some cases, reach stressed levels at the maximum allowable load, such as branches 26–25, 14–15 and 24–22. They approach the stability limit (1.00) in the remaining cases.

The *NCPI* is consistent with the other indices for branch 9–11 since the line resistance of this branch is zero. From Table 3, it is also noted that the *NCPI* is largely consistent with *FVSI* in most cases because of heavy reactive power since the variations are only for the reactive power.

As a result, the proposed index presents an accurate instrument for voltage instability prediction. Figure 7 depicts the maximum allowable reactive power load in each specific bus, with the load buses sorted in ascending order. The bar chart in Fig. 7 illustrates the weak and robust areas in the power system.

The area that includes buses 25, 26, 27, 29 and 30 is considered the weakest area in the system since these buses carry the minimum allowable loads in the system. It is interesting to note that although bus 28 is connected to the weak area, it is a robust bus since it is supplied by reactive power from the generator at bus 8 as shown in Fig. 4. The area, which includes load buses 3, 4, 6, 7, 9 and 12, has been identified as a robust area because of high allowable reactive power loadings. This is because this area is surrounded by generator buses, as shown in Fig. 4. The results demonstrate that the suggested index is capable of determining the weak buses and areas of power systems.

Figure 8 shows the variations of line voltage stability indices during reactive power variations at bus-26. It can be seen that the curve of *NCPI* is almost the same as the *FVSI*. This is because the active power is very small in comparison to the reactive power. The *NCPI* and *FVSI* have high performance, and their curves are semi-linear.

Figure 8 also shows that *NCPI* and *FVSI* approach 0.8 when the reactive power increases to 28 MVAr, and voltage collapse occurs when reactive power increases to 31.5 MVAr. The operator should take safe space from the voltage collapse point and take quicker preventive action in time to avoid voltage instability.

6.1.1.4 Heavy active and reactive power loading It is commonly recognized that simultaneous active and reactive power load variations are more likely to occur in practical power systems. Heavy active and reactive power loads are added on the specific load buses of the IEEE 30-bus system, as depicted in Table 4, to examine the capability of the proposed index. From Table 4, the *NCPI* approaches unity at each critical active and reactive power loading.

Table 4 shows that the proposed index is closer to 1.00 than the other stability indices, while L_{mn} and *FVSI* fail to detect the critical branches. However, L_{mn} diagnoses the line 7–5 as a critical line, while *FVSI* diagnoses line 7–5 as a stressed line. This is because L_{mn} has an indirect relation with the active power through the voltage angle difference, and the voltage angle difference is high in this case. The *FVSI* is a simplified equation form of L_{mn} when the angle is ignored, as illustrated in Sect. 2.2. Therefore, the *FVSI* fails to detect these critical branches because of ignoring the difference in voltage angles.
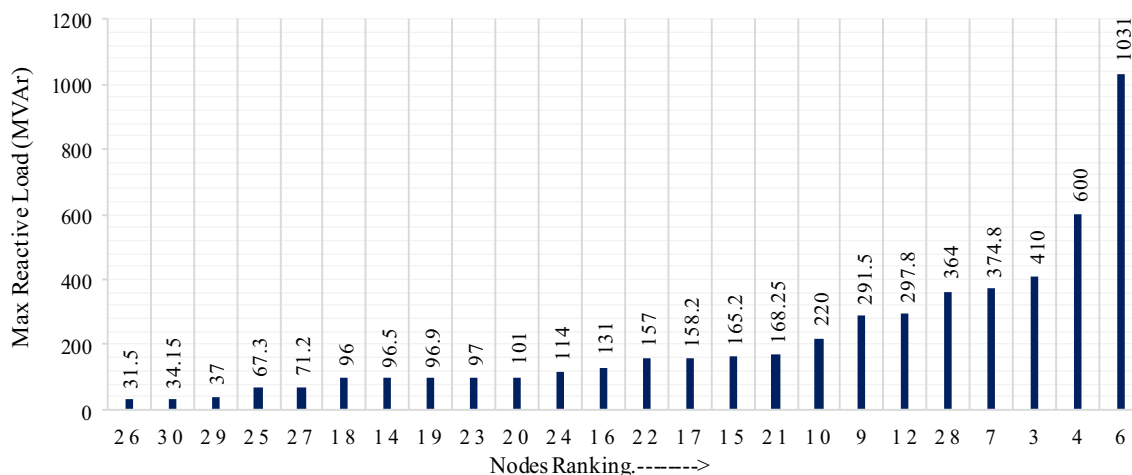

Fig. 7 Maximum permitted reactive power loading (MVAr) of the load buses in the IEEE 30-bus
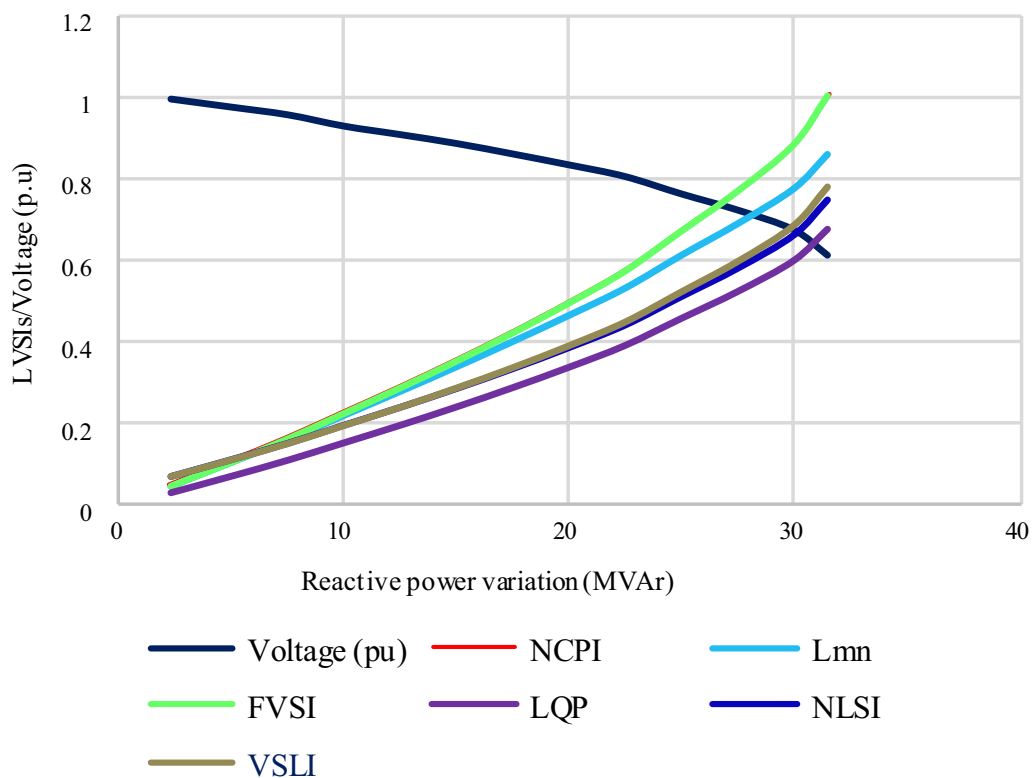
Fig. 8 Variations of line voltage stability indices (LVSIs) for branch 26–25 during reactive power variations at bus 26

Table 4 Heavy active and reactive power at some load buses of the IEEE 30-bus test system

Bus no.	Apparent power P(MW) Q(MVAr)	Most critical lines	Lines (from–to)	NCPI	L_{mn}	FVSI	LQP	NLSI	VSLI
Bus-3	P = 290 Q = 265	3–1	3–1	0.9481	0.6522	0.3578	0.2836	0.6487	0.9494
			3–4	0.6205	0.6095	0.6019	0.5159	0.6214	0.6218
Bus-7	P = 381 Q = 200	7–5	7–5	0.9795	0.9580	0.8389	0.5348	0.9624	0.9853
			7–6	0.7386	0.5016	0.2872	0.3148	0.6553	0.8738
Bus-12	P = 212 Q = 174	12–4	12–4	0.9743	0.2363	0.1459	0.9641	0.1459	0.9361
			12–13	0.8993	0.8993	0.8993	0.8993	0.8993	0.8993
			12–16	0.0286	0.0662	0.0577	0.1126	0.2750	0.3272
			12–15	0.0275	0.0095	0.0089	0.0195	0.1028	0.1149
			12–14	0.0681	0.0684	0.0672	0.0551	0.0317	0.0304
Bus-14	P = 89 Q = 64.6	14–15	14–15	0.9903	0.7340	0.5822	0.1143	0.8653	0.8817
			14–12	0.9143	0.8922	0.7541	0.4067	0.9251	0.9566
Bus-24	P = 86 Q = 77.3	24–22	24–22	0.9540	0.7852	0.6789	0.3275	0.8558	0.9047
			24–23	0.7137	0.6762	0.6102	0.3925	0.7464	0.7658
			24–25	0.6323	0.5839	0.5218	0.3040	0.6796	0.6986
Bus-30	P = 27 Q = 25.9	30–27	30–27	0.9828	0.8982	0.7633	0.3899	0.9324	0.9577
			30–29	0.6980	0.6598	0.6060	0.3901	0.7242	0.7367

One interesting factor to be noted in this case is that the *NLSI* shows high values when the active and reactive power flow is in the same direction, such as branches 7–5, 14–15, 24–22 and 30–27. Conversely, the *LQP* shows low values for these branches. On the other hand, the *LQP* shows a high value for branch 12–4 when the active and reactive power is in the opposite direction, whereas the *NLSI* shows a low value for this branch. Thus, the directions of power flow play a critical role in determining the voltage collapse accurately. It is noted that the *NLSI* fails to predict the critical branches 3–1, 14–15 and 24–22, although the directions of power are the same. This is because the formulation of the *NLSI* still has a sensitive assumption where the index ignores the voltage angle difference.

Note that *VSLI* approaches 1.00 in most cases. However, the *VSLI* reaches a stressed level for branches 14–15 and 24–22.

Figure 9 represents the variations of voltage and line voltage stability indices (LVSIs) for line 14–15 during the variation of apparent power (MVA), which is gradually increased with the same power factor (0.812). It is noted that the *NCPI* approaches the stability limit when the apparent power load reaches the critical level. Branch 14–15 is identified as the most critical line by the proposed index. In contrast, the other LVSIs fail to approach the stability limit. Therefore, the proposed index shows a high performance and is more effective than other indices in the presence of active and reactive power variations.

6.1.2 IEEE 118-bus test system

The proposed index is examined on the large IEEE 118-bus system to investigate its practicability and versatility. The bus and line data of the IEEE 118-bus system are available in [85], and the line diagram is shown in Fig. 5. The system is examined during several operating conditions as follows.

6.1.2.1 Base case loading   To prove the versatility of the proposed index, it is also evaluated on a large grid for the base case. Table 5 presents the results of the simulation studies. The proposed index and indices *LQP*, *NLSI* and *VSLI* have the highest values for the line connected between buses 25 and 27. Therefore, line 25–27 is the weakest line based on these indices under the base case loading. The proposed index and *NLSI* identify line 38–65 as the second weakest line, while L_{mn} and *FVSI* identify this branch as the weakest line in the system. However, the *NCPI* has a value higher than other indices for this line.

The results show that the proposed index, in most cases, is close to the values of indices L_{mn}, *FVSI* and *LQP*, while the proposed index is slightly higher than L_{mn}, *FVSI* and *LQP*. This is because the proposed index takes into
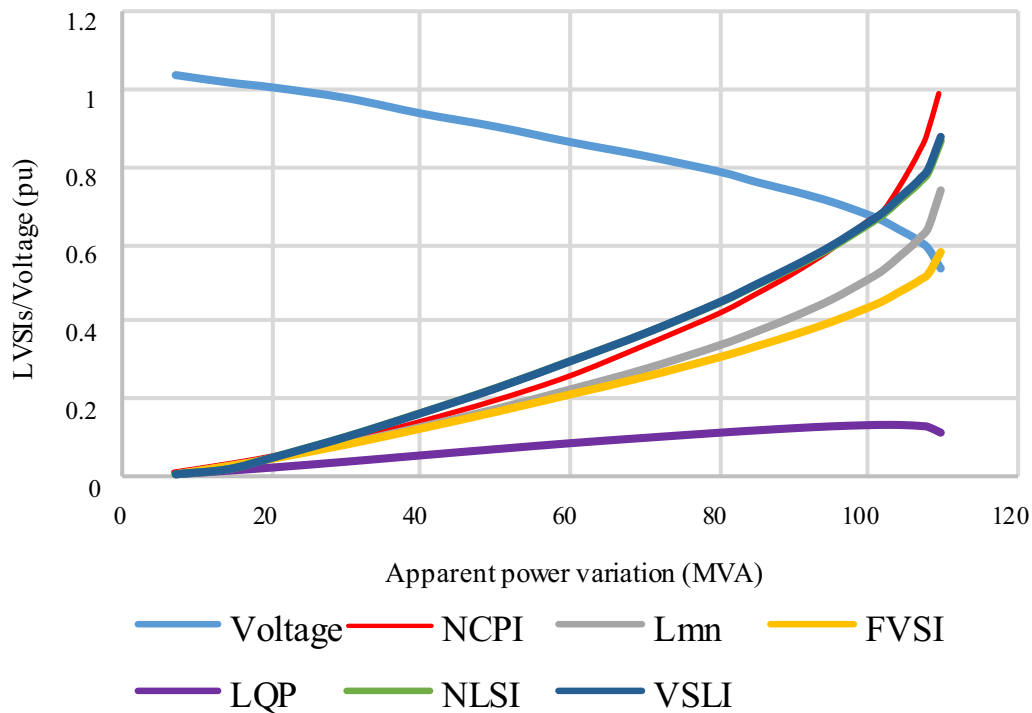

Fig. 9 Variations of line voltage stability indices (LVSIs) for branch 14–15 during apparent power variations at bus 14

Table 5 The line stability indices for the IEEE 118-bus for the base case loading

Line (from–to)	NCPI	L_{mn}	FVSI	LQP	NLSI	VSLI
13–15	0.0434	0.0433	0.0434	0.0396	0.0375	0.0069
25–23	0.2022	0.1213	0.1252	0.1884	0.2248	0.1756
47–49	0.0283	0.0282	0.0281	0.0256	0.0327	0.0307
38–65	0.3499	0.2382	0.2223	0.0905	0.2852	0.2205
25–27	0.4254	0.2092	0.2170	0.4074	0.4038	0.2877
55–59	0.1029	0.0802	0.0770	0.0491	0.1409	0.1401
59–63	0.1094	0.0941	0.0938	0.0782	0.0998	0.0609
66–65	0.1034	0.1034	0.1034	0.1034	0.1034	0.1871
69–68	0.1559	0.1526	0.1524	0.1438	0.1524	0.1267
77–76	0.2499	0.1887	0.1970	0.2223	0.2833	0.2767
99–80	0.1095	0.1052	0.1036	0.0933	0.1311	0.1141
101–100	0.1252	0.1219	0.1233	0.1160	0.0995	0.0945

account the directions of active and reactive power flow, and the line resistance is not entirely ignored. The values of the *NLSI* and *VSLI* are close to each other in most cases, while the value of the proposed index is consistent with the values of other indices where the branches have zero resistance, such as branches 59–63, 66–65 and 69–68. When line resistance is not considered, active power flow in the line has no impact on line voltage drop, making the *NCPI* values almost the same as with the values of the other indices. When line resistance is considered in the squared term of line impedance, as shown in the formulation of the *NCPI*, the results from the case mentioned above indicate that the suggested index is better and more accurate than other indices for predicting the stressed condition of a line.

6.1.2.2 Heavy active power loading Heavy active power loading is applied on the IEEE 118-bus system to prove the versatility and capability of the proposed index. The active power loading is increased until the power flow fails to give any solution. The load is critical in this case, and the line stability indices should approach 1.00. Otherwise, the stability indices fail to detect voltage instability.

The results in Table 6 show high performance of the proposed index due to heavy active power loading, and approaches 1.00 in each specific bus loading. The indices L_{mn}, *FVSI* and *NLSI* fail to detect the critical lines in each case. This is because the L_{mn} and *FVSI* ignore the influence of active power on formulating their indices. Also, the *FVSI* and *NLSI* ignore the voltage angle difference.

It can be seen that the *LQP* index surpasses the stability limit (1.00) in some instances, such as branches 13–15, 51–49 and 67–66, denoting that the collapse had already happened. This is because the index *LQP* entirely ignores line resistance and this causes errors in collapse

prediction. It is noted that the *VSLI* fails to diagnose the voltage collapse of branch 17–30 because of massive active power applied on bus 17. The results of the case studies mentioned above provide credibility in the practicability on a large grid that the suggested index is better than other indices in terms of accuracy and precision for predicting the critical state of a line.

6.1.2.3 Heavy reactive power loading Heavy reactive power loadings are applied on the large IEEE 118-bus test system at each specific load bus to validate the proposed index's practicability. Table 7 represents the results of case studies for selected load buses due to space restrictions. Table 7 shows that the proposed index approaches unity when the reactive power loading reaches the maximum allowable load. Further increase of reactive load at these buses leads to the divergence of the power flow solution, and this denotes that the load is critical and closes to the voltage instability point. It is noted that the proposed index is the closest index to 1.00.

The index *LQP* shows lower values for branches 117–12, 38–65 and 51–49. This denotes that the loading margin is still available, and the collapse may occur if the lines are further loaded. This is because the *LQP* index entirely ignores line resistance and doesn't consider the direction of power flow.

The indices *NLSI* and *VSLI* reach stressed levels for branches 117–12 and 33–37 when the reactive loadings reach the critical level on load buses 117 and 33. It can be seen that L_{mn} and *FVSI* have high response because of heavy reactive power. However, the proposed index is closer to the stability limit than the other stability indices. The proposed index offers a more accurate collapse prediction than the other indices on the voltage stability of a line.

Table 6 The line stability indices for the IEEE 118-bus system under heavy active power load

Bus No	Active power (MW)	Most Critical lines	Lines (from-to)	NCPI	L_{mn}	FVSI	LQP	NLSI	VSLI
Bus-13	500	13–15	13–15	1.0043	0.6722	0.2437	1.2909	0.2751	0.9904
			13–11	0.7460	0.2414	0.1401	0.4783	0.5245	0.8220
Bus-17	1014	17–30	17–30	0.9332	0.4395	0.3954	0.9032	0.3954	0.0979
			17–113	0.2336	0.2316	0.2295	0.2064	0.2459	0.2462
			17–16	0.1278	0.1134	0.1096	0.0863	0.1671	0.1651
			17–31	0.1162	0.0148	0.0131	0.0835	0.1904	0.2658
			17–15	0.0409	0.0269	0.0258	0.0368	0.0442	0.0540
			17–18	0.0408	0.0386	0.0381	0.0335	0.0601	0.0608
Bus-20	396.8	20–19	20–19	0.9721	0.5477	0.2854	0.7570	0.6897	0.9860
			20–21	0.5292	0.3222	0.2648	0.5240	0.0412	0.2246
Bus-51	466	51–49	51–49`	0.9637	0.7095	0.2064	1.2640	0.3610	0.9981
			51–58	0.3480	0.1705	0.1361	0.0819	0.4109	0.5594
			51–52	0.1473	0.1234	0.1165	0.0779	0.2123	0.2301
Bus-67	695	67–66	67–66	0.9389	0.2999	0.1076	1.1730	0.2696	0.9281
			67–62	0.8464	0.3211	0.1762	0.5484	0.4856	0.8950

Table 7 The line stability indices for the IEEE 118-bus system under heavy reactive power load

Bus no.	Reactive power (MVAr)	Most critical lines	Lines (from–to)	NCPI	L_{mn}	FVSI	LQP	NLSI	VSLI
Bus-117	152	117–12	117–12	0.9995	0.9778	0.9952	0.8987	0.8932	0.9010
Bus-20	230	20–19	20–19	1.0102	0.9898	1.0102	0.9682	0.9765	0.9846
			20–21	0.5412	0.5379	0.5349	0.5036	0.5439	0.5418
Bus-38	1020	38–65	38–65	1.0030	1.0413	0.9287	0.8074	0.9667	0.9775
			38–30	0.9787	0.9776	0.9558	0.9621	0.9558	0.9616
			38–37	0.9407	0.9275	0.9085	0.8764	0.9005	0.9375
Bus-51	329.5	51–49	51–49	1.0103	1.0015	1.0013	0.8245	1.0001	0.9980
			51–58	0.8185	0.7711	0.8180	0.7262	0.7117	0.7326
			51–52	0.4541	0.4215	0.4440	0.3904	0.3348	0.3584
Bus-33	300	33–37	33–37	1.0046	0.9656	1.0023	0.9068	0.9122	0.8992
			33–15	1.0017	0.9553	1.0010	0.8036	0.8815	0.9023
Bus-96	685	96–80	96–80`	0.9998	0.9737	0.9855	0.9360	0.9696	0.9648
			96–94	0.7963	0.7714	0.7953	0.7213	0.7444	0.7488
			96–97	0.7596	0.7480	0.7562	0.7261	0.7381	0.7378
			96–82	0.7588	0.7351	0.7584	0.6912	0.7046	0.7088

6.1.2.4 Heavy active and reactive power loading In order to prove the versatility and capability of the proposed index, heavy active and reactive power loadings are applied at specific load buses of the IEEE 118-bus system, as shown in Table 8. Practical power systems have high probability of active and reactive power variations. Additionally, the loading MVA margin can be determined in different power factors for each bus to avoid voltage collapse.

The results in Table 8 indicate that the proposed index approaches unity at each particular load bus. This

property is unavailable in other stability indices. It is noted that the index L_{mn} approaches the stability limit for branches 117–12 and 50–49 and approaches the stressed level for branch 96–80, since L_{mn} has an indirect relation with the active power through the voltage angle difference. *FVSI* is a simplified form of L_{mn} and ignores the voltage angle difference. Therefore, the *FVSI* fails to diagnose these branches as critical lines. The erroneous collapse prediction occurs since L_{mn} and *FVSI* ignore the effect of active power flow. The index *LQP* fails to detect the critical branches in each critical load because of

Table 8 The line stability indices for the IEEE 118-bus system under heavy apparent power load

Bus no.	Apparent power P (MW), Q (MVAr)	Most critical lines	Lines (from–to)	NCPI	L_{mn}	FVSI	LQP	NLSI	VSLI
Bus-117	P = 137 Q = 106.2	117–12	117–12	0.9817	0.9405	0.7088	0.3653	0.8758	0.9792
Bus-20	P = 180 Q = 165	20–19	20–19	0.9789	0.8961	0.7869	0.5942	0.8934	0.9005
			20–21	0.3478	0.2937	0.2721	0.1847	0.3734	0.3857
Bus-30	P = 920 Q = 710	30–26	30–26	0.9834	0.7737	0.5941	0.2027	0.6971	0.8922
			30–8	0.8230	0.8191	0.8067	0.7812	0.8225	0.8042
			30–38	0.8988	0.8868	0.6292	0.8722	0.4665	0.3874
			30–17	0.5861	0.5844	0.5839	0.5818	0.5839	0.6663
Bus-50	P = 300 Q = 278	50–49	50–49	0.9920	0.9556	0.7231	0.3302	0.9220	0.9906
			57–50	0.8579	0.8419	0.7866	0.6057	0.8670	0.8691
Bus-96	P = 570 Q = 490	96–80	96–80	0.9562	0.8734	0.6384	0.2567	0.8097	0.9958
			96–94	0.7479	0.7312	0.6866	0.5546	0.7664	0.7809
			96–97	0.6940	0.6077	0.5230	0.3136	0.6595	0.7790
			96–82	0.6460	0.5950	0.5230	0.3474	0.6744	0.7325

heavy active and reactive power loadings. This is because the index *LQP* entirely ignores line resistance and doesn't consider the directions of active and reactive power flow.

The index *NLSI* approaches the stressed level in most cases and achieves a stability limit for branch 50–49. This is because the index *NLSI* ignores the voltage angle difference and doesn't consider the direction of power flow. The index *VSLI* approaches stability limits in most cases and reaches a stressed level for branches 20–19 and 30–26.

As a result, the proposed index provides a more precise collapse prediction in a large grid when there are active and reactive power variations than the other stability indices.

6.2 Contingency ranking and analysis

The stressed loadings and unpredictable incidents in a power system, termed contingencies, cause voltage violations. Contingencies in a power system can occur because of the line outages contingency (LOC) or generator outages contingency (GOC). Both single (N-1) and multiple contingencies (N-k) are possible in the system. Contingency analysis and voltage collapse prediction are carried out simultaneously since contingency is one of the participating reasons for voltage violation in a power system. This method helps power system operators determine the most affected lines when one of the generators or lines is separated from the system for maintenance or exposing the system to an external disturbance under different operating conditions. The most sensitive lines need accurate monitoring, control, protection and immediate correction. Voltage stability and contingency

analysis is performed on the IEEE 30-bus and the large IEEE 118-bus test systems.

6.2.1 IEEE 30-bus test system

The contingency ranking and analysis are performed on IEEE 30-bus test system in the following conditions.

6.2.1.1 Base case loading with one-line outage Contingency ranking and analysis are carried out under base load to assess the performance of the proposed index in collapse prediction during a line outage. The load flow is conducted with a line outage at a time under the base case loading, and the index *NCPI* is computed and compared with the well-known stability indices for verification. The line interruption causes other overloaded lines, which become stressed or critical lines. The line with the highest value of *NCPI* is considered the most stressed line.

Table 9 shows the results of contingency ranking and analysis under the base case loadings obtained from different line outages in the system. An outage of line 1–2 causes the *NCPI* to increase to 1.2539 for line 1–3, indicating that the system is unstable. Line 1–3 will be interrupted because of the interruption of line 1–2, and in this case, the generated active power at generator-1 increases by 18.2% (from 260.99 to 308.5 MW).

Also, the generated reactive power increases significantly (118%) to preserve bus voltages within permitted limits. Because of the overloading caused by the outage of line 1–2, the power loss on line 1–3 also significantly increases from 2.808 to 40.997 MW. The line diagram in Fig. 4 shows that the interruption of line 1–2 from the system makes line 1–3 carry all the generated power

Table 9 Contingency ranking and analysis of the IEEE 30-bus system under the base case loadings

Line outage	Rank of lines outages	Rank of each outage	Most stressed lines	NCPI	L_{mn}	FVSI	LQP	NLSI	VSLI
1–2	1	1	3–1	1.2539	1.1654	0.5855	1.5824	0.1194	0.8707
		2	4–2	0.3550	0.3148	0.3322	0.2832	0.2103	0.2327
		3	9–11	0.2011	0.2011	0.2011	0.2011	0.2011	0.2011
		4	6–4	0.1990	0.1834	0.1740	0.1806	0.0879	0.0872
4–6	2	1	6–2	0.2620	0.1677	0.1447	0.2372	0.0731	0.1714
		2	5–2	0.2451	0.1200	0.1052	0.2367	0.0688	0.1884
		3	9–11	0.1391	0.1391	0.1391	0.1391	0.1391	0.1391
12–15	3	1	12–4	0.1494	0.1169	0.1160	0.1494	0.1160	0.1868
		2	9–11	0.1240	0.1240	0.1240	0.1240	0.1240	0.1240
29–27	4	1	30–27	0.1205	0.0907	0.0836	0.0405	0.2243	0.2419
		2	28–27	0.0920	0.0721	0.0718	0.0515	0.0718	0.0428
15–18	5	1	9–11	0.1168	0.1168	0.1168	0.1168	0.1168	0.1168
		2	20–10	0.0523	0.0486	0.0475	0.0361	0.0912	0.0936
30–29	6	1	28–27	0.0870	0.0673	0.0670	0.0469	0.0670	0.0480
		2	30–27	0.0803	0.0597	0.0559	0.0277	0.1728	0.1849

from generator-1. All these factors indicate that the system is unstable in this condition. For the same line, the indices *FVSI* and *NLSI* are far away from the stability limit, whereas L_{mn} and *LQP* diagnose the system as unstable. *LQP* increases to 1.5824 while *NLSI* is 0.1194. This is because the active and reactive power flows are in the opposite directions. In addition, the index *LQP* ignores the losses (40.997 MW), which makes its value very high. *VSLI* diagnoses line 1–3 as the most stressed line with a value of 0.8707.

It is interesting to observe that the results show line 9–11 as one of the most stressed lines in most cases. This is because line 9–11 is connected as a radial design, and the synchronous condenser provides additional reactive power to compensate for the reactive power losses due to line outages. The reactive power flow increases in branch 9–11 and becomes one of the most stressed lines. The remaining contingencies are ranked as shown in Table 9.

6.2.1.2 Pre-specified reactive power loading with one line outage A pre-specified load is chosen as half of the maximum allowable reactive power loading of the load bus on the basis of [67]. Half of the maximum allowable reactive power loads obtained from Fig. 7 are applied on buses 12, 20 and 30, as shown in Table 10. The other load buses stay constant as in the base case loading.

The load flow is run with N-1 contingency (single line outage), as illustrated in Table 10. The most sensitive line due to a line outage has the highest value of *NCPI*, and is considered a critical line when *NCPI* approaches 1.00. Based on the *NCPIs*, the line outage that leads the other lines to approach collapse is classified in the first rank in

terms of the risk of its interruption from the system. It is seen that interruption of line 29–27 leads to the highest *NCPI* of 0.9461 for branch 30–27. Therefore, the interruption of line 29–27 is classified as the first rank. This is to be expected since buses 30 and 27 have low reactive power margins, as shown in Fig. 7. The other index values approach 0.9 except *LQP*, which determines the line as a healthy line. *LQP* shows a lower value for the interruption of line 29–27, which illustrates that the contingency is not critical.

It is interesting to note that *LQP* reaches the stressed level for branch 12–13 since the line resistance is zero, while it fails to identify the critical and stressed lines in the remaining cases.

As a result, the proposed index shows an effective performance and accuracy compared to other stability indices.

6.2.1.3 Prespecified loading with a generation unit outage Pre-specified loadings are set at half of the maximum allowable reactive power loading of the load bus on the basis of [67]. Contingency analysis is conducted in the system to observe the effect of a generation unit outage. Contingency ranking and analysis are performed by eliminating a generation unit in sequence for every prespecified case shown in Table 11a, b and c. The load flow calculation is run with one generation unit outage at a time, and there is no need to increase the reactive loading in the system. The load buses are randomly selected to justify the risk of generator outages that may occur in the system. The most sensitive lines are sorted in descending order from every generator outage, as shown in Table 11.

Table 10 Contingency ranking and analysis of the IEEE 30-bus system with pre-specified reactive power load

Line outage	Rank of lines outages	Rank of each outage	Most stressed lines (from–to)	NCPI	L_{mn}	FVSI	LQP	NLSI	VSLI
29–27	1	1	30–27	0.9461	0.9005	0.8518	0.5430	0.8988	0.9001
		2	12–4	0.6731	0.6231	0.6129	0.5527	0.6129	0.4069
		3	28–27	0.5775	0.5433	0.5364	0.4953	0.5364	0.4602
12–4	2	1	12–13	0.8242	0.8242	0.8242	0.8242	0.8242	0.8242
		2	6–10	0.6013	0.4775	0.4565	0.3118	0.4565	0.4825
30–29	3	1	30–27	0.8146	0.7742	0.7592	0.5326	0.7871	0.7878
		2	12–4	0.6694	0.6213	0.6115	0.5536	0.6115	0.4032
		3	28–27	0.5122	0.4805	0.4753	0.4384	0.4753	0.3922
20–19	4	1	20–10	0.6797	0.6421	0.6795	0.5645	0.5771	0.5901
		2	12–4	0.6632	0.6067	0.5956	0.5282	0.5956	0.3948

Prespecified reactive power load: Q12 = 148.9 MVAr, Q20 = 50.5MVAr, Q30 = 17.1 MVAr

Table 11 Contingency ranking and analysis of the IEEE 30-bus system with pre-specified reactive power load at (a) buses 4, 7, 9, 16 and 20, (b) nodes 4 and 16, (c) nodes 7 and 28

Generator outage	Rank	Most stressed lines	NCPI	L_{mn}	FVSI	LQP	NLSI	VSLI
(a) Prespecified reactive power load: Q4 = 205 MVAr, Q7 = 187.5 MVAr, Q9 = 145.8 MVAr, Q16 = 65.5 MVAr, Q20 = 50.5 MVAr								
Gen. 5	1 (Critical)	8–6	0.9441	0.9429	0.9022	0.8376	0.8108	0.7862
	2 (Critical)	9–11	0.9003	0.9003	0.9003	0.9003	0.9003	0.9003
	3 (Stressed)	16–12	0.8569	0.7988	0.8530	0.6849	0.7445	0.7575
	4	7–6	0.7544	0.7374	0.7468	0.6625	0.7267	0.7260
	5	20–10	0.7438	0.7101	0.7371	0.6030	0.6751	0.6799
	6	4–2	0.6352	0.6172	0.5829	0.4709	0.6617	0.6684
(b) Prespecified reactive power load: Q4 = 205MVAr, Q16 = 65.5MVAr								
Gen. 13	1 (Most stressed)	4–12	0.8565	0.7663	0.7511	0.8565	0.7511	0.2716
	2	16–17	0.5193	0.4947	0.5191	0.4386	0.4273	0.4387
	3	4–2	0.4616	0.4478	0.4292	0.3564	0.4941	0.4948
	4	16–12	0.4511	0.4374	0.4491	0.3641	0.4006	0.4033
(c) Prespecified reactive power load: Q7 = 187.5 MVAr, Q28 = 181.5 MVAr								
Gen. 8	1 (Critical)	7–5	0.9497	0.8733	0.9492	0.8180	0.8049	0.8355
	2	10–6	0.7839	0.6804	0.6666	0.7839	0.6666	0.7038
	3	28–6	0.7142	0.6988	0.7131	0.6575	0.6777	0.6719
	4	28–8	0.5989	0.5816	0.5989	0.5436	0.5438	0.5389

The generator outage that causes the *NCPI* value for any branch to increase to the highest-level approaching 1.00 is considered the most severe contingency. The contingency is applied in different system areas to validate the proposed index versatility. From Table 11, the following analysis and observations can be concluded.

- Case 1 (Table 11a)

The results show that the proposed index increases to a critical level and approaches 0.9441 for branch 8–6 because of generator-5 outage and pre-specified reactive power loadings at nodes 4, 7, 9, 16 and 20. The index L_{mn} verifies this as it also increases to 0.9429. The other stability indices reach the stressed level, but *VSLI* is far from the critical value (1.00). Line 9–11 is also identified as the most critical line by the proposed index, and its value is consistent with all the other stability indices. The indices values for branch 9–11 reach 0.9003. Therefore, branches 8–6 and 9–11 are identified as the most critical lines due to the outage of generator-5. They are sorted in the first two-line ranks, considered the most severe

contingency. The results are to be expected since the generators at node-8 and node-11 provide heavy reactive power through lines 8–6 and 9–11. Thus lines 8–6 and 9–11 become the most critical lines. The line ranks based on their closeness to the voltage collapse points due to the contingency are sorted in descending order, as shown in the second column of Table 11a.

- Case 2 (Table 11b)

In this case, the outage of generator 13 (N-1) leads to an outage of line 13–12 (N-2) since the load is zero at node 13, and the line becomes an open circuit. The results show that the proposed index increases to a stressed level and approaches 0.8565 for branch 4–12 because of the outage of generator 13 and pre-specified reactive power loads at nodes 4 and 16. Again the results are expected since line 4–12 carries large reactive power from generators 1 and 2 because of the outage of generator 13. The value of index *LQP* is consistent with the proposed index since the resistance of branch 4–12 is zero. Because of the outage of generator 13, the other indices, especially *VSLI*, offer a minimum value that diagnoses the contingency as not critical.

- Case 3 (Table 11c)

The results show that the proposed index increases to a critical level and approaches 0.9497 for branch 7–5 because of the outage of generator-8 and pre-specified reactive power loadings at nodes 7 and 28. It is also an expected result since generator-5 provides more reactive power through line 7–5, and the line becomes the most

critical one in the system. The index *FVSI* verifies the practicability of the proposed index, increasing to 0.9492 for branch 7–5. The other indices diagnose line 7–5 as a stressed line. The most sensitive line rankings due to the outage of generator-8 are tabulated in the second column of Table 11c.

According to the above contingencies cases, it can be deduced that the proposed index accurately predicts the critical states of lines due to the contingency, which can help the system dispatchers to make an appropriate rectification on time to avoid voltage collapse.

6.2.2 IEEE 118-bus test system

The *NCPI* is further investigated on a large IEEE 118-bus test system under double line outages (N-2) and double generation unit outages (N-2) contingencies. The results are analyzed and compared with those achieved by indices L_{mn}, *FVSI*, *LQP*, *NLSI* and *VSLI* to prove the versatility of the proposed index. Contingency analysis is carried out under a predetermined load to examine the effectiveness of the suggested index for envisioning voltage collapse during double line outages (N-2) and double generation unit outages (N-2).

6.2.2.1 Line contingency (N-2) analysis Predetermined reactive power loads are applied on buses 11, 20, 30, 33, 51, 75 and 96, as shown in Table 12. The other load buses stay constant as in the base case loading. The load flow is run with a double line removed (N-2) in the system, and the results of the proposed index *NCPI* are evaluated and compared with those obtained by L_{mn}, *FVSI*, *LQP*, *NLSI*

Table 12 Contingency ranking and analysis of the IEEE 118-bus system with two lines outages and pre-specified reactive power load at nodes 11, 20, 30, 33, 51, 75 and 96

Pre-specified reactive power load: Q11 = 872 MVAr, Q20 = 115, Q30 = 700 MVAr, Q33 = 150MVAr, Q51 = 165 MVAr, Q75 = 550MVAr, and Q96 = 343 MVAr

Lines outages (N-2)	The rank of lines outages	Rank of each outage	Most stressed lines (from–to)	NCPI	L_{mn}	FVSI	LQP	NLSI	VSLI
96–97 75–74	1	1	75–70	0.9377	0.8722	0.9311	0.8523	0.8077	0.8437
		2	75–69	0.9356	0.9230	0.8815	0.7099	0.9330	0.9271
		3	75–77	0.9079	0.8871	0.8966	0.7985	0.8808	0.8722
		4	96–80	0.7021	0.6973	0.6987	0.6673	0.6951	0.6842
		5	30–26	0.7007	0.6297	0.5840	0.4560	0.6419	0.6382
30–8 96–82	2	1	30–26	0.8981	0.8586	0.7896	0.6618	0.8435	0.8516
		2	96–80	0.7343	0.7286	0.7314	0.6991	0.7249	0.7146
		3	75–69	0.6635	0.6355	0.5812	0.4369	0.6950	0.7072
75–69 13–11	3	1	30–26	0.7011	0.6330	0.5882	0.4642	0.6451	0.6378
		2	75–77	0.6747	0.6334	0.5766	0.4340	0.6925	0.7085
		3	96–80	0.5691	0.5663	0.5657	0.5405	0.5669	0.5544

and *VSLI*. The critical lines are determined based on the *NCPI*, whose interruptions initiate the process of collapse.

Line contingencies (N-2) are ranked in descending order based on the *NCPI* as shown in Table 12. The line outages (N-2) that expose other lines in proximity to the voltage collapse point (1.00) are ranked first in terms of the risk of their interruption. Table 12 shows that interruption of branches 96–97 and 75–74 increases the proposed index to the critical level for branches 75–70, 75–69 and 75–77, with the corresponding *NCPI* values increased to 0.9377, 0.9356 and 0.9079, respectively. It is noted that the *FVSI* values verify the proposed index value for branches 75–70 and 75–77, while the indices L_{mn}, *NLSI* and *VSLI* verify the proposed index value for branch 75–69.

One interesting factor, in this case, is that the index *LQP* shows the lowest performance of the stability indices, especially for branches 75–69 and 75–77. This erroneous collapse prediction of *LQP* occurs because of the entirely ignored line resistance. *LQP* also shows the minimum value for all the remaining contingencies, which denotes healthy voltage stable states. The value of the proposed index approximates the stability limit equal to 0.8981 for branch 30–26 due to outages of branches 30–8 and 96–82. The indices L_{mn}, *NLSI* and *VSLI*, are close to the proposed index value, while *FVSI* and *LQP* show the lowest value compared to the other indices.

Interruption of lines 96–97 and 75–74 is the most critical contingency, while the contingency due to the interruption of lines 30–8 and 96–82 is in the second rank. The results are also expected since the interruption of

line 75–74 prevents generator 74 from providing reactive power to bus 75 as shown in Fig. 5. Bus 96 is still robust since it is in the vicinity of the shunt compensation at bus 82, which provides reactive power to bus 96, as shown in the bus data in [85].

Moreover, generator-8 provides reactive power to bus 30 through line 30–8. The interruption of this line prevents the generator at bus 8 from supporting reactive power to bus 30. Thus, the proposed index is able to monitor the unsafe conditions of transmission lines for any contingency or disturbance. This can assist operators in implementing appropriate rectification to circumvent the voltage collapses. The results indicate that the proposed index adapts to different contingencies, while this property is unavailable in other stability indices.

6.2.2.2 Generator contingency (N-2) analysis Contingency analysis is conducted to verify the regularity of the outage contingency ranking by simulating two generator outages (N-2) in the power system for different pre-specified states. The proposed index is used as an instrument to determine the criticalness of a specific line when a generator outage occurs in the power system. Table 13 shows that the outage of generators at nodes 8 and 74 is considered the most severe contingency since it leads to increased *NCPI* values to stressed levels for branches 75–69 and 75–70. The contingency due to outages of generators 76 and 99 is in the second rank in terms of severity. It is noted that L_{mn}, *NLSI* and *VSLI* verify the values of *NCPI* and identify the contingency due to the outage of generators 8 and 74 as the most severe contingency. It is

Table 13 Contingency ranking and analysis of the IEEE 118-bus system with two generator outages and pre-specified reactive power load at nodes 11, 20, 30, 33, 51, 75 and 96

Pre-specified reactive power load: Q11 = 872 MVAr, Q20 = 115, Q30 = 700 MVAr, Q33 = 150MVAr, Q51 = 165 MVAr, Q75 = 550MVAr, and Q96 = 343 MVAr

Generator outages (N-2)	The rank of generator outages	Rank of lines	Most stressed lines (from–to)	NCPI	L_{mn}	FVSI	LQP	NLSI	VSLI
Gen. 8	1	1	75–69	0.8599	0.8344	0.7755	0.6047	0.8607	0.8635
Gen. 74		2	75–70	0.7939	0.7620	0.7933	0.7257	0.7219	0.7296
		3	30–26	0.7534	0.6889	0.6375	0.5087	0.6947	0.6945
Gen. 76	2	1	75–69	0.7290	0.6846	0.6278	0.4769	0.7359	0.7460
Gen. 99		2	75–77	0.7116	0.6847	0.7112	0.6522	0.6402	0.6409
		3	30–26	0.7014	0.6275	0.5805	0.4482	0.6396	0.6398
Gen. 15	3	1	30–26	0.7208	0.6498	0.6010	0.4690	0.6596	0.6605
Gen. 19		2	75–69	0.6666	0.6392	0.5852	0.4411	0.6977	0.7094
		3	33–37	0.6240	0.6156	0.6179	0.5610	0.6113	0.6045
Gen. 54	4	1	30–26	0.7016	0.6272	0.5801	0.4472	0.6394	0.6401
Gen. 56		2	75–69	0.6671	0.6401	0.5865	0.4432	0.6980	0.7091
		3	51–49	0.6148	0.6017	0.5825	0.4833	0.6306	0.6293

noted that *LQP* shows the lowest values in all contingency analyses because of its entirely ignored line resistance. It is seen that the branches 30–26 and 75–69 are the most sensitive lines for each contingency. Although bus 96 is near generators 76 and 99, their outages do not affect the branches connected to bus 96, and thus bus 96 is a robust bus for each contingency. The results show that the proposed index has a higher performance in determining the system contingency risks than other stability indices.

7 Conclusions

This paper proposes a novel collapse prediction index (*NCPI*) for voltage stability assessment, and contingency ranking and analysis in power systems. The practicability and performance of the proposed index have been investigated on the IEEE 30-bus system and the large IEEE 118-bus system under various operating conditions. The results have been compared with the most important voltage stability indices. The results in all operational circumstances clearly highlight the superior accuracy and efficacy of the proposed method for voltage stability assessment. This is because the proposed index takes into account many considerations for formulation, namely:

- The proposed index does not ignore the effect of active power, as do the indices L_{mn} and *FVSI*.
- The proposed index strongly relates to active and reactive power variations, as shown in (24).
- The proposed index does not ignore the voltage angle difference, as do indices *FVSI* and *NLSI*. Ignoring voltage angle difference creates erroneous collapse prediction error when the angle is high because of a heavily loaded line.
- The proposed index's formulation is based on only partially ignoring the line resistance since entirely ignoring line resistance creates an enormous error in collapse prediction, as in the *LQP* which shows the lowest performance. In addition, the *LQP* assumes the lines as lossless, leading to inaccurate collapse prediction, while the *LQP* surpasses the stability limit in some cases because of this omission. The proposed index considers the line resistance in terms of line impedance squared. This supports the index value so as not to affect the process of the proposed index formulation.
- The proposed index takes into account the influence of active and reactive power flow directions, which play an essential role in precisely detecting the voltage collapse points.

The *NCPI* can identify voltage collapse brought on by heavy active power, reactive power, and apparent power load. This feature is unavailable in other voltage stability indices. The results under all power system operations and contingencies show that the proposed index can identify the weak buses as well as the load ranking in the power system and determine the critical lines referred to a bus. The voltage stability analysis identifies the weak buses and critical lines referred to a bus and buses ranking, whereas the contingency analysis identifies the most critical line or generator outages in the power system. The proposed index has been used for both analyses and has shown effective performance during all operational circumstances.

The proposed index can determine the critical outage and the voltage collapse points. It can be used to perform meticulous contingency ranking and analysis. It can be used as an effective tool for contingency analysis since it can provide a priori prediction of the critical or stressed conditions of transmission lines and the weak area of the system accurately when single or multiple contingencies occur in the power system. The proposed index values have been sorted in descending order for each outage of line or generator (N-1 or N-2) to identify the severity of the contingency. The results have been compared with the well-known stability indices for verification purposes.

The comprehensive implementation results on two IEEE test systems illustrate that this novel collapse prediction index is significantly better than the other stability indices. The *NCPI* may offer a promising instrument for voltage stability assessment, and contingency ranking and analysis under all operational circumstances.

8 Future work

This work can be extended to the use of the proposed index for security and stability constraint optimal power flow (SSCOPF) to obtain minimum cost, loss and the *NCPI* index, and satisfy all operational constraints. Also, equality and inequality constraints should be added to these equations. A system using this technique will be more economical, reliable, stable and secure.

Abbreviations

L_{mn}	Line stability indicator
FVSI	Fast voltage stability index
LQP	Line stability factor
NLSI	New line stability index
VSLI	Voltage stability line index
NVSI	New voltage stability index
NCPI	Novel collapse prediction index
LVSIs	Line voltage stability indices
VSIs	Voltage stability indices
CBI	Critical boundary index
NR	Newton Raphson

L(i)	Line number and i = 1,2,… number of lines in the power grid
G(i)	Generators number where i = 1,2,… number of generators in the power grid
LF	Load flow

Acknowledgements

Author contributions

Authors' Information

Salah Mokred received a bachelor's degree in electric power systems and machines from Sana'a University, Yemen, and M.Sc. degree from North China Electric Power University (NCEPU), China. After graduation with a B.S. degree, he worked as a teaching assistant at Sana'a University for 2 years. He is currently a Ph.D. student at Southeast University, Nanjing, China. His research interest includes power system operation, stability, analysis and planning. Salah Mokred received a bachelor's degree in electric power systems and machines from Sana'a University, Yemen, and M.Sc. degree from North China Electric Power University (NCEPU), China. After graduation with a B.S. degree, he worked as a teaching assistant at Sana'a University for 2 years. He is currently a Ph.D. student at Southeast University, Nanjing, China. His research interest includes power system operation, stability and planning.
Yifei Wang received the M.Sc. degree in electrical engineering from Wuhan University, and the Ph.D. degree in electrical engineering from Zhejiang University. He was a postdoc with the Electrical and Computer Engineering Department, Illinois Institute of Technology. He is currently an Assistant Professor with the School of Electrical Engineering, Southeast University, Nanjing, China. His research interests include convex optimization in power systems, power system operation and economics.
Tiancong Chen received the M.Sc. degree in Henan University of Science and Technology. She is now an assistant professor with the School of Eletromechanical Engineering, Zhongyuan Institute of Science and Technology, Zhengzhou, China. Her research interests include power system analysis and operation and power system security.

Funding

Availability of data and materials

The data of IEEE 30-bus and IEEE 118-bus test systems are available in reference [85]

Declarations

Competing interests

The authors declare that they have no known competing financial interests or personal relationships that could have appeared to influence the work reported in this paper.

References

1. DHAL. (2016). Voltage stability assessment using equivalent nodal analysis. *IEEE Transactions on Power System, 31*(1), 454–463.
2. Aldeen, M., Saha, S., Alpcan, T., & Evans, R. J. (2015). New online voltage stability margins and risk assessment for multi-bus smart power grids. *International Journal of Control, 88*(7), 1338–1352.
3. Moradi, R. A., & Zeinali Davarani, R. (2021). Introducing a new index to investigate voltage stability of power systems under actual operating conditions. *International Journal of Electrical Power & Energy Systems, 136*(September 2021), 107637. https://doi.org/10.1016/j.ijepes.2021.107637
4. Soyemi, A., Misra, S., Oluranti, J., & Ahuja, R., et al. (2022). Evaluation of voltage stability indices. In L. Garg, N. Kesswani, & J. G. Vella (Eds.), *Information systems and management science. ISMS 2020. Lecture notes in networks and systems.* (Vol. 303). Cham: Springer. https://doi.org/10.1007/978-3-030-86223-7_8
5. Kundur, P. (1994) *Power system stability and control.* Columbia, British.
6. Naik, S. D., Khedkar, M. K., & Bhat, S. S. (2014). Effect of line contingency on static voltage stability and maximum loadability in large multi bus power system. *International Journal of Electrical Power & Energy Systems, 67*, 448–452. https://doi.org/10.1016/j.ijepes.2014.12.002
7. Vournas, C. D., Nikolaidis, V. C., & Tassoulis, A. A. (2006). Postmortem analysis and data validation in the wake of the 2004 Athens blackout. *IEEE Transactions on Power Systems, 21*(3), 1331–1339. https://doi.org/10.1109/TPWRS.2006.879252
8. Andersson, G., et al. (2005). Causes of the 2003 major grid blackouts in North America and Europe, and recommended means to improve system dynamic performance. *IEEE Transactions on Power Systems, 20*(4), 1922–1928. https://doi.org/10.1109/TPWRS.2005.857942
9. Lee, C. Y., Tsai, S. H., & Wu, Y. K. (2010). A new approach to the assessment of steady-state voltage stability margins using the P-Q-V curve. *International Journal of Electrical Power & Energy Systems, 32*(10), 1091–1098. https://doi.org/10.1016/j.ijepes.2010.06.005
10. Overbye, T. J. (1994). Effects of load modelling on analysis of power system voltage stability. *International Journal of Electrical Power & Energy Systems, 16*(5), 329–338. https://doi.org/10.1016/0142-0615(94)90037-X
11. Nagendra, P., Nee Dey, S. H., & Paul, S. (2011). An innovative technique to evaluate network equivalent for voltage stability assessment in a widespread sub-grid system. *International Journal of Electrical Power & Energy Systems, 33*(3), 737–744. https://doi.org/10.1016/j.ijepes.2010.11.024
12. Chebbo, A. M., Irving, M. R., & Sterling, M. J. H. (1992). Voltage collapse proximity indicator: Behaviour and implications. *IEE Proceedings-C, 139*(3), 241–252.
13. Mohammadi, H., Khademi, G., Dehghani, M., & Simon, D. (2018). Voltage stability assessment using multi-objective biogeography-based subset selection. *International Journal of Electrical Power & Energy Systems, 103*(June), 525–536. https://doi.org/10.1016/j.ijepes.2018.06.017
14. Jasmon, G. B., Callistus, L. H., & Lee, C. (1991). Prediction of voltage collapse in power systems using a reduced system model. In *International conference on control 1991, IET* (pp. 32–36).
15. Tiwari, R., Niazi, K. R., & Gupta, V. (2012). Line collapse proximity index for prediction of voltage collapse in power systems. *International Journal of Electrical Power & Energy Systems, 41*(1), 105–111. https://doi.org/10.1016/j.ijepes.2012.03.022
16. Ismail, N. A. M., Zin, A. A. M., Khairuddin, A., & Khokhar, S. (2014). A comparison of voltage stability indices. In *Proceedings of the 2014 IEEE 8th international power engineering and optimization conference. PEOCO 2014* (No. March, pp. 30–34). https://doi.org/10.1109/PEOCO.2014.6814394.
17. Babu, R., Raj, S., Dey, B., & Bhattacharyya, B. (2022). Optimal reactive power planning using oppositional grey wolf optimization by considering bus vulnerability analysis. *Energy Conversion and Economics, 3*(1), 38–49. https://doi.org/10.1049/enc2.12048
18. Ajjarapu, V., & Lee, B. (1992). Bifurcation theory and its application to nonlinear dynamical phenomena in an electrical power system. *IEEE Transactions on Power Systems, 7*(1), 424–431. https://doi.org/10.1109/59.141738
19. Gao, B., Morison, G. K., & Kundur, P. (1992). Voltage stability evaluation using modal analysis. *IEEE Power Engineering Review, 12*(11), 41. https://doi.org/10.1109/MPER.1992.161430
20. Abdalla Seedahmed, M. M., Sofyan Mokred, S. A., & Kamara, G. (2019). Voltage stability estimation for complex power system based on modal analytical techniques. In *2019 6th international conference on signal processing and integrated networks, SPIN 2019* (pp. 1035–1041). https://doi.org/10.1109/SPIN.2019.8711683.

21. Canizares, C. A., De Souza, A. C. Z., & Quintana, V. H. (1996). Comparison of performance indices for detection of proximity to voltage collapse. *IEEE Transactions on Power System, 11*(3), 1441–1450. https://doi.org/10.1109/59.535685

22. Caizares, C. A. (1995). On bifurcations, voltage collapse and load modeling. *IEEE Transactions on Power Systems, 10*(1), 512–522. https://doi.org/10.1109/59.373978

23. Löf, P. A., Smed, T., Andersson, G., & Hill, D. J. (1992). Fast calculation of a voltage stability index. *IEEE Transactions on Power Systems, 7*(1), 54–64. https://doi.org/10.1109/59.141687

24. Gadal, R., Elmariami, F., Oukennou, A., Agouzoul, N., & Tarraq, A. (2022). An assessment of line voltage stability indices to select the best combination for voltage stability prediction. In *The proceedings of the international conference on electrical systems & automation*. Singapore: Springer. https://doi.org/10.1007/978-981-19-0035-8.

25. Pattabhi, M. B., Lakshmikantha, B. R., & Sundar, K. S. (2022). A novel method for contingency ranking based on voltage stability criteria in radial distribution systems. *Technology and Economics of Smart Grids and Sustainable Energy*. https://doi.org/10.1007/s40866-022-00137-y

26. Kessel, P., & Glavitsch, H. (1986). Estimating the voltage stability of a power system. *IEEE Transactions on Power Delivery, PWRD-1*(3), 346–354.

27. Hongjie, J., Xiaodan, Y., & Yixin, Y. (2005). An improved voltage stability index and its application. *International Journal of Electrical Power & Energy Systems, 27*(8), 567–574. https://doi.org/10.1016/j.ijepes.2005.08.012

28. Hagmar, H., Tong, L., Eriksson, R., & Tuan, L. A. (2021). Voltage instability prediction using a deep recurrent neural network. *IEEE Transactions on Power Systems, 36*(1), 17–27. https://doi.org/10.1109/TPWRS.2020.3008801

29. Kumar, S., Tyagi, B., Kumar, V., & Chohan, S. (2022). PMU-based voltage stability measurement under contingency using ANN. *IEEE Transactions on Instrumentation and Measurement, 71*, 1–11. https://doi.org/10.1109/TIM.2021.3129210

30. Devaraj, D., & Preetha Roselyn, J. (2011). On-line voltage stability assessment using radial basis function network model with reduced input features. *International Journal of Electrical Power & Energy Systems, 33*(9), 1550–1555. https://doi.org/10.1016/j.ijepes.2011.06.008

31. Alhamrouni, I., Alif, M. A., Ismail, B., Salem, M., Jusoh, A., & Sutikno, T. (2018). Load flow based voltage stability indices for voltage stability and contingency analysis for optimal location of STATCOM in distribution network with integrated distributed generation unit. *Telkomnika (Telecommunication Computing Electronics and Control), 16*(5), 2302–2315. https://doi.org/10.12928/TELKOMNIKA.v16i5.10577

32. Pulok, M. K. H., & Faruque, M. O. (2015). Utilization of PMU data to evaluate the effectiveness of voltage stability boundary and indices. In *2015 North American power symposium, NAPS 2015* (No. 1, pp. 9–14). https://doi.org/10.1109/NAPS.2015.7335111.

33. Alshareef, A., Shah, R., Mithulananthan, N., & Alzahrani, S. (2021). A new global index for short term voltage stability assessment. *IEEE Access, 9*, 36114–36124. https://doi.org/10.1109/ACCESS.2021.3061712

34. Esmaili, M., Firozjaee, E. C., & Shayanfar, H. A. (2014). Optimal placement of distributed generations considering voltage stability and power losses with observing voltage-related constraints. *Applied Energy, 113*, 1252–1260. https://doi.org/10.1016/j.apenergy.2013.09.004

35. Sadeghi, S. E., & Akbari Foroud, A. (2021). A general index for voltage stability assessment of power system. *International Transactions on Electrical Energy Systems*. https://doi.org/10.1002/2050-7038.13155

36. Modarresi, J., Gholipour, E., & Khodabakhshian, A. (2016). A comprehensive review of the voltage stability indices. *Renewable and Sustainable Energy Reviews, 63*, 1–12. https://doi.org/10.1016/j.rser.2016.05.010

37. Nageswa Rao, A. R., Vijaya, P., & Kowsalya, M. (2021). Voltage stability indices for stability assessment: A review. *International Journal of Ambient Energy, 42*(7), 829–845. https://doi.org/10.1080/01430750.2018.1525585

38. Danish, M. S. S., Senjyu, T., Danish, S. M. S., Sabory, N. R., Narayanan, K., & Mandal, P. (2019). A recap of voltage stability indices in the past three decades. *Energies, 12*(8), 1–19. https://doi.org/10.3390/en12081544

39. Furukakoi, M., et al. (2018). Electrical power and energy systems critical boundary index (CBI) based on active and reactive power deviations. *Electrical Power and Energy Systems, 100*(May 2017), 50–57. https://doi.org/10.1016/j.ijepes.2018.02.010

40. Ratra, S., Tiwari, R., & Niazi, K. R. (2018). Voltage stability assessment in power systems using line voltage stability index. *Computers & Electrical Engineering, 70*, 199–211. https://doi.org/10.1016/j.compeleceng.2017.12.046

41. Salama, H. S., & Vokony, I. (2022). Voltage stability indices—a comparison and a review. *Computers & Electrical Engineering, 98*, 107743. https://doi.org/10.1016/j.compeleceng.2022.107743

42. Amroune, M., Bourzami, A., & Bouktir, T. (2014). Weakest buses identification and ranking in large power transmission network by optimal location of reactive power supports. *TELKOMNIKA: Indonesian Journal of Electrical Engineering, 12*(10), 7123–7130. https://doi.org/10.11591/telkomnika.v12i8.6421

43. Moger, T., & Dhadbanjan, T. (2015). A novel index for identification of weak nodes for reactive compensation to improve voltage stability. *IET Generation, Transmission & Distribution, 9*, 1826–1834. https://doi.org/10.1049/iet-gtd.2015.0054

44. Ren, C., Xu, Y., Zhang, Y., & Zhang, R. (2020). A hybrid randomized learning system for temporal-adaptive voltage stability assessment of power systems. *IEEE Transactions on Industrial Informatics, 16*(6), 3672–3684. https://doi.org/10.1109/TII.2019.2940094

45. Dharmapala, K. D., Rajapakse, A., Narendra, K., & Zhang, Y. (2020). Machine learning based real-time monitoring of long-term voltage stability using voltage stability indices. *IEEE Access, 8*, 222544–222555. https://doi.org/10.1109/ACCESS.2020.3043935

46. Ramirez, L., & Dobson, I. (2014). Monitoring voltage collapse margin by measuring the area voltage across several transmission lines with synchrophasors. In *IEEE power & energy society general meeting* (Vol. 2014-Octob, No. October, pp. 0–4). https://doi.org/10.1109/PESGM.2014.6938974.

47. Kamel, M., Member, S., Karrar, A. A., & Eltom, A. H. (2018). Development and application of a new voltage stability index for on-line monitoring and shedding. *IEEE Transactions on Power Systems, 33*(2), 1231–1241. https://doi.org/10.1109/TPWRS.2017.2722984

48. Guddanti, K. P., Matavalam, A. R. R., & Weng, Y. (2020). PMU-based distributed non-iterative algorithm for real-time voltage stability monitoring. *IEEE Transactions on Smart Grid, 11*(6), 5203–5215. https://doi.org/10.1109/TSG.2020.3007063

49. Fan, Y., Liu, S., Member, S., Qin, L., Li, H., & Qiu, H. (2015). A novel online estimation scheme for static voltage stability margin based on relationships exploration in a large data set. *IEEE Transactions on Power Systems, 30*(3), 1380–1393. https://doi.org/10.1109/TPWRS.2014.2349531

50. Gao, P., Shi, L., Yao, L., Ni, Y., & Bazargan, M. (2009). Multi-criteria integrated voltage stability index for weak buses identification. In, T D Asia 2009 (pp. 1–5). https://doi.org/10.1109/TD-ASIA.2009.5356950.

51. Babu, R., Raj, S., & Bhattacharyya, B. (2020). Weak bus-constrained PMU placement for complete observability of a connected power network considering voltage stability indices. *Protection and Control of Modern Power Systems, 5*, 1. https://doi.org/10.1186/s41601-020-00174-8

52. Xi, L., Li, H., Zhu, J., Li, Y., & Wang, S. (2022). A novel automatic generation control method based on the large-scale electric vehicles and wind power integration into the grid. *IEEE Transactions on Neural Networks and Learning Systems*. https://doi.org/10.1109/TNNLS.2022.3194247

53. Xie, L., Wu, J., Li, Y., Sun, Q., & Xi, L. (2022). Automatic generation control strategy for integrated energy system based on ubiquitous power internet of things. *IEEE Internet of Things Journal*. https://doi.org/10.1109/jiot.2022.3209792

54. Mokred, S., Lijun, Q., Kamara, G., & Khan, T. (2020). Comparison of the effect of series and shunt capacitor application in 25kV radial power distribution network. In *2020 IEEE/IAS industrial and commercial power system Asia*, ICPS Asia 2020 (pp. 822–830). https://doi.org/10.1109/ICPSAsia48933.2020.9208355.

55. Mokred, S., Lijun, Q., & Kamara, G. (2020). Smart design of distribution series capacitor bank application for improved voltage quality and motor start. In *2020 IEEE/IAS industrial and commercial power system Asia*, ICPS Asia 2020 (No. 1, pp. 454–459). https://doi.org/10.1109/ICPSAsia48933.2020.9208381.

56. Mokred, S., Lijun, Q., & Khan, T. (2021). Transient and protection performance of a fixed series compensated 500 kV transmission line during various types of faulty conditions. *Journal of Electrical Engineering & Technology*. https://doi.org/10.1007/s42835-020-00646-9

57. Mokred, S., Lijun, Q., & Khan, T. (2020). Protection performance during application of an intelligent and fast switch series capacitor to 25kV radial power distribution network. In 2020 *IEEE/IAS industrial and commercial*

power system Asia, ICPS Asia 2020 (pp. 921–928). https://doi.org/10.1109/ICPSAsia48933.2020.9208391.

58. Thasnas, N., & Siritaratiwat, A. (2019). Implementation of static line voltage stability indices for improved static voltage stability margin. *Journal of Electrical and Computer Engineering*. https://doi.org/10.1155/2019/2609235

59. Khunkitti, S., et al. (2019). A comparison of the effectiveness of voltage stability indices in an optimal power flow. *IEEJ Transactions on Electrical and Electronic Engineering, 14*(4), 534–544. https://doi.org/10.1002/tee.22836

60. Kyomugisha, R., Muriithi, C. M., & Nyakoe, G. N. (2022). Performance of various voltage stability indices in a stochastic multiobjective optimal power flow using mayfly algorithm. *Journal of Electrical and Computer Engineering, 2022*, 6–8. https://doi.org/10.1155/2022/7456333

61. Khunkitti, S., & Premrudeepreechacharn, S. (2020). Voltage stability improvement using voltage stability index optimization. In *Proceedings of 2020 international conference on power, energy and innovations, ICPEI 2020* (Vol. 2, No. 2, pp. 193–196). https://doi.org/10.1109/ICPEI49860.2020.9431536.

62. Matsukawa, Y., Watanabe, M., Wahab, N. I. A., & Othman, M. L. (2019). Voltage stability index calculation by hybrid state estimation based on multi objective optimal phasor measurement unit placement. *Energies*. https://doi.org/10.3390/en12142688

63. Duman, S., Li, J., & Wu, L. (2021). AC optimal power flow with thermal–wind–solar–tidal systems using the symbiotic organisms search algorithm. *IET Renewable Power Generation*. https://doi.org/10.1049/rpg2.12023

64. Adewuyi, O. B., Howlader, H. O. R., Olaniyi, I. O., Konneh, D. A., & Senjyu, T. (2020). Comparative analysis of a new VSC-optimal power flow formulation for power system security planning. *International Transactions on Electrical Energy Systems, 30*(3), 1–16. https://doi.org/10.1002/2050-7038.12250

65. Kyomugisha, R., Muriithi, C. M., & Edimu, M. (2021). Multiobjective optimal power flow for static voltage stability margin improvement. *Heliyon, 7*(12), e08631. https://doi.org/10.1016/j.heliyon.2021.e08631

66. Moghavvemi, M., & Omar, F. M. (1998). Technique for contingency monitoring and voltage collapse prediction. *IEE Proceedings - Generation, Transmission and Distribution, 145*, 634–640. https://doi.org/10.1049/ip-gtd:19982355

67. Musirin, I., & Rahman, T. K. A. (2002). On-line voltage stability based contingency ranking using fast voltage stability index (FVSI). In Transmission and Distribution Conference and Exhibition 2002. AsiaPacific (pp. 1118-1123). https://doi.org/10.1109/TDC.2002.1177634.

68. Mohamed, A., & Jasmon, G. B. (1998). A static voltage collapse indicator using line stability factors. *Journal of Industrial Technology, 7*(1), 73–85.

69. Yazdanpanah-Goharrizi, A., & Asghari, R. (2007). A novel line stability index (NLSI) for voltage stability assessment of power systems. In *International conference on power system, Beijing, China* (pp. 164–167).

70. Kanimozhi, R., & Selvi, K. (2013). A novel line stability index for voltage stability analysis and contingency ranking in power system using fuzzy based load flow. *Journal of Electrical Engineering and Technology*. https://doi.org/10.5370/JEET.2013.8.4.694

71. Abdulrahman, T. K., & Jasmon, G. B. (1995). A new technique for voltage stability analysis in a power system and improved loadflow algorithm for distribution network. In *International conference on energy management and power delivery, EMPD '95* (pp. 714–719). https://doi.org/10.1109/EMPD.1995.500816.

72. Tran, M. T. (2009). Definition and implementation of voltage stability indices in PSS ® NETOMAC master of science thesis in electric power engineering definition and implementation of voltage stability indices in PSS ® NETOMAC conducted at Siemens AG.

73. Wondie, T. T., & Tella, T. G. (2022). Voltage stability assessments and their improvement using optimal placed static synchronous compensator (STATCOM). *Journal of Electrical and Computer Engineering, 2022*, 1–12. https://doi.org/10.1155/2022/2071454

74. Goh, H. H., Chua, Q. S., Lee, S. W., Kok, B. C., Goh, K. C., & Teo, K. T. K. (2015). Evaluation for voltage stability indices in power system using artificial neural network. *Procedia Engineering, 118*, 1127–1136. https://doi.org/10.1016/j.proeng.2015.08.454

75. Samy, K. A., & Venkadesan, A. (2021). Online assessment of voltage stability region using an artificial neural network. In *2021 5th international*

conference on electrical, electronics, communication, computer technologies and optimization techniques, ICEECCOT 2021—proceedings (No. December, pp. 757–761). https://doi.org/10.1109/ICEECCOT52851.2021.9708047.

76. Meena, M. K., & Kumar, N. (2018). On-line monitoring and simulation of transmission line network voltage stability using FVSI. In *2018 2nd IEEE international conference on power electronics, intelligent control and energy systems, ICPEICES 2018* (Vol. 3, pp. 257–260). https://doi.org/10.1109/ICPEICES.2018.8897403.

77. Chandra, A., & Pradhan, A. K. (2019). Online voltage stability assessment using wide area measurements. In *2019 8th international conference on power systems, transition towards sustainable, smart and flexible grids, ICPS 2019*. https://doi.org/10.1109/ICPS48983.2019.9067663.

78. Chintakindi, R., & Mitra, A. (2021). Detecting weak areas in a real-time power system on a static load model using standard line voltage stability indices. In *Proceedings of the 2021 IEEE 2nd international conference on smart technologies for power, energy and control, STPEC 2021* (pp. 0–5). https://doi.org/10.1109/STPEC52385.2021.9718768.

79. Yari, S., & Khoshkhoo, H. (2019). A comprehensive assessment to propose an improved line stability index. *International Transactions on Electrical Energy Systems, 29*(4), 1–25. https://doi.org/10.1002/etep.2806

80. Yari, S., & Khoshkhoo, H. (2017). Assessment of line stability indices in detection of voltage stability status. In *Conference. Proceedings—2017 17th IEEE international conference on environment and electrical engineering and 2017 1st IEEE industrial and commercial power systems Europe, EEEIC/ICPS Europe*, 2017 (pp. 7–11). https://doi.org/10.1109/EEEIC.2017.7977454.

81. Hussian, F., Goyal, G. R., Arya, A. K., & Soni, B. P. (2021). Contingency ranking for voltage stability in power system. In *Proceedings. CONECCT 2021 7th IEEE international conference on electronics, computing and communication technologies* (pp. 12–15). https://doi.org/10.1109/CONECCT52877.2021.9622724.

82. Subramani, C. et al. (2009). Line outage contingency screening and ranking for voltage stability assessment. In *International conference on power system, Kharagpur, India* (pp. 1–5). https://doi.org/10.1109/ICPWS.2009.5442743.

83. Dobson, I., Parashar, M., & Carter, C. (2010). Combining phasor measurements to monitor cutset angles. In *Proceedings of the annual Hawaii international conference on system sciences* (pp. 1–9). https://doi.org/10.1109/HICSS.2010.110.

84. Moghavvemi, M., & Faruque, M. O. (2001). Technique for assessment of voltage stability in ill-conditioned radial distribution network. *IEEE Power Engineering Review*. https://doi.org/10.1109/39.893345

85. Power System Test Archive-UWEE, University of Washington. http://www.ee.washington.edu/research/pstca.